Chapter 4

Weak Interactions

4.1 LEPTONIC, SEMILEPTONIC, AND NONLEPTONIC INTERACTIONS

The observed weak interactions can be subdivided into three types; leptonic, semileptonic, and nonleptonic. As the name implies, the purely leptonic weak interactions involve only electrons, muons, and neutrinos. Only one example, that of muon decay, has been observed so far:

$$\mu^+ \rightarrow e^+ + \nu_e + \bar{\nu}_\mu,$$

and

$$\mu^- \rightarrow e^- + \bar{\nu}_e + \nu_\mu.$$

The necessity of postulating two types of neutrinos, ν_e and ν_μ, and their antiparticles was mentioned in Section 1.3.2 and is discussed in detail in Section 4.9. The leptonic weak interactions, as we shall see, are distinguished by the fact that they obey the pure V-A theory. The semileptonic weak interactions involve both leptons and hadrons, strange or nonstrange. Examples are nuclear β-decay,

$$n \rightarrow p + e^- + \bar{\nu}_e,$$

the inverse process of neutrino absorption by a nucleon,

$$\nu_e + n \rightarrow p + e^-,$$

pion decay,

$$\pi^+ \rightarrow \mu^+ + \nu_\mu,$$

and the β-decay of the Λ-hyperon,

$$\Lambda \rightarrow p + e^- + \bar{\nu}_e.$$

Finally, the nonleptonic weak interactions occur between hadrons only.

They always involve a change of strangeness of the hadron, $|\Delta S| = 1$. For example,

$$K^+ \to \pi^+ + \pi^+ + \pi^-,$$

and

$$\Lambda \to p + \pi^-.$$

Nonleptonic weak interactions between nonstrange hadrons must also take place. Thus, two nucleons undergo a specifically weak interaction, but it is feeble in comparison with the strong interaction. Only in those cases where a strong interaction is forbidden (when the strangeness changes) can the nonleptonic weak interactions be observed experimentally.

All the weak interactions involve decay lifetimes or collision cross sections typical of the weak coupling (Fermi) constant, $G = 10^{-5}/M_p^2$. We have already mentioned the smallness of this constant, and remarked that, in the weak process of muon capture by a nucleus,

$$\mu^- + p \to n + \nu_\mu,$$

the mean free path of the muon in nuclear matter is of order 10^{14} times the characteristic nuclear scale of length (10^{-13} cm). Quite out of context, we may note however that, on a cosmic scale, the Fermi constant plays an important role in determining the evolutionary rate of young dwarf stars like the sun, and its smallness has, in a very real sense, guaranteed the long life of the solar system. Thermonuclear energy is released in the sun by the conversion of hydrogen to helium via the p–p cycle:

$$\begin{aligned} \mathrm{H}^1 + \mathrm{H}^1 &\to \mathrm{H}^2 + e^+ + \nu \qquad (10^9 \text{ yr}), \\ \mathrm{H}^2 + \mathrm{H}^1 &\to \mathrm{He}^3 + \gamma \qquad (1 \text{ sec}), \\ \mathrm{He}^3 + \mathrm{He}^3 &\to \mathrm{He}^4 + \mathrm{H}^1 + \mathrm{H}^1 \qquad (10^6 \text{ yr}). \end{aligned}$$

The overall rate of these reactions is determined by that of the first and slowest step (the estimated mean reaction time in the solar core being given in brackets), and this depends very largely on the magnitude of the β-decay constant, G. It may also be remarked that recent experiments to detect solar neutrinos underground have confirmed the correctness of the above reactions as the solar energy source, on the basis of a null result. (See Problem 4.10.)

4.2 NUCLEAR β-DECAY; A BRIEF REVIEW

The first weak interaction process to be observed was nuclear β-decay. The salient observations were:

a) e^+ and e^- are emitted by radioactive nuclei. The lifetimes are very long (second-years) compared with the nuclear time scale (10^{-22} sec).

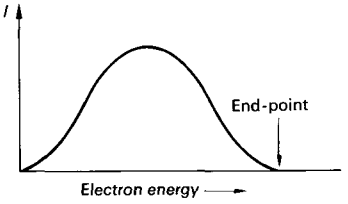

Fig. 4.1 Typical shape of electron energy spectrum in nuclear β-decay ("allowed" transition).

b) The electron (or positron) energy spectrum is continuous (Fig. 4.1). The total disintegration energy (as measured by the masses of parent and daughter nuclei) is discrete, and corresponds to the maximum possible energy of the electrons (the end-point of the spectrum).

c) Conservation of energy, momentum, and angular momentum require the existence of a light, uncharged particle of spin $\frac{1}{2}$, called a *neutrino* (Pauli, 1933), and its antiparticle, the antineutrino. Careful measurement of the recoil momentum of the daughter nucleus, as well as the electron energy, established that the neutrino mass was nearly zero (i.e. $E_\nu \simeq cp_\nu$).

d) The independent existence of neutrinos was demonstrated by Reines and Cowan in 1953–59, in experiments using the intense $\bar{\nu}$-fluxes from a reactor (see Section 4.10).

e) The prototype β-interactions are described by the equations

$$n \rightarrow p + e^- + \bar{\nu}, \qquad \text{negatron emission (i)},$$

$$p \rightarrow n + e^+ + \nu, \qquad \text{positron emission (ii)},$$

$$e^- + p \rightarrow n + \nu, \qquad K\text{-capture (iii)},$$

$$\bar{\nu} + p \rightarrow n + e^+, \qquad \text{antineutrino absorption (iv)}.$$

Reaction (i) occurs for free neutrons (mean lifetime $\tau \sim 10$ min), (ii) occurs only in nuclei where the difference in binding between parent and daughter nuclei exceeds the negative Q-value of the reaction. K-capture (iii) occurs chiefly in heavy nuclei as an alternative to positron emission, or where positron emission is forbidden energetically.

4.2.1 Fermi and Gamow-Teller Transitions

The so-called "allowed" β-transitions are those in which the electron and neutrino carry off zero orbital angular momentum ($l = 0$). Their total angular momentum is then 1 (spins parallel) or 0 (spins antiparallel). The two cases are referred to as Gamow-Teller and Fermi transitions respectively. If we call

J the nuclear angular momentum, we have, indicating spin directions symbolically by vertical arrows:

Fermi	Gamow-Teller
$n \to p + e^- + \bar{\nu}$	$n \to p + e^- + \bar{\nu}$
$\uparrow \quad \uparrow \quad \downarrow \quad \uparrow$	$\uparrow \quad \downarrow \quad \uparrow \quad \uparrow$
$\Delta J = 0$	$\Delta J = 1 (\lvert\Delta J\rvert = 0, \pm 1)$
$J_i = 0 \to J_f = 0$ allowed.	$J_i = 0 \to J_f = 0$ forbidden.

There are then three types of allowed β-transitions; pure Fermi, pure Gamow-Teller, and mixed transitions. Examples are:

	$He^6 \to Li^6 + e^- + \bar{\nu}$;	$\Delta J = 1$;	pure Gamow-Teller,
J^P	$0^+ \quad 1^+$		
	$O^{14} \to N^{14*} + e^+ + \nu$;	$J = 0 \to J = 0$;	pure Fermi,
J^P	$0^+ \quad 0^+$		
	$n \to p + e^- + \bar{\nu}$;	$J \to J (J \neq 0)$;	mixed.
J^P	$\frac{1}{2}^+ \quad \frac{1}{2}^+$		

Note that in all cases, the parity of the initial and final nuclear states is the same. The effect of the decay is to flip the isospin of one nucleon ($n \to p$ or vice versa), and, in the Gamow-Teller case, also to flip the nucleon spin, but otherwise to leave the nuclear configuration unaltered.

4.2.2 Fermi Theory of β-decay—the Phase-Space Factor

Since the interaction is known to be weak, the transition probabilities for β-decays can be calculated from first order perturbation theory. The transition probability per unit time is then (Section 3.4)

$$W = \frac{2\pi}{\hbar} G^2 |M|^2 \frac{dN}{dE_0}, \tag{4.1}$$

where E_0 is the available energy of the final state, dN/dE_0 is the density of final states per unit energy, and G^2 is a universal constant typical of the β-decay coupling. $|M|^2$ is the square of the matrix element for the transition, which involves an integral over the nuclear (interaction) volume of the four fermion wave functions. For the present we shall regard $|M|^2$ as some constant and calculate the phase-space factor dN/dE_0. This is determined by the number of ways it is possible to share out the available energy $E_0 \to E_0 + dE_0$ between, for example, p, e^-, and $\bar{\nu}$ in the neutron decay (i) above. The quantity dE_0 arises because of the spread in energy of the final state, corresponding to the

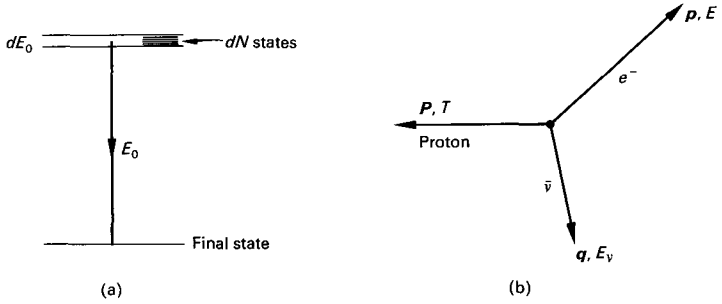

Fig. 4.2 (a) An initial state with a spread in energy dE_0 decays to a final (stable) state of unique energy, with energy release E_0. (b) The momentum vectors in neutron β-decay.

finite lifetime of the initial state. In Fig. 4.2, $\boldsymbol{p}$, $\boldsymbol{q}$, and $\boldsymbol{P}$ are the momentum of the electron, neutrino, and proton; E, E_ν, and T are their kinetic energies.

Then, in the rest frame of the initial state (neutron):

$$\boldsymbol{P} + \boldsymbol{q} + \boldsymbol{p} = 0,$$
$$T + E_\nu + E = E_0.$$

Assume $m_\nu = 0$, so $E_\nu = qc$. In order of magnitude, $E_0 \sim 1$ MeV, so $Pc \sim 1$ MeV. Thus, if the recoiling nucleon mass is M, its kinetic energy $T = P^2/2M \simeq 10^{-3}$ MeV only, and can be neglected. The nucleon serves to conserve momentum, but we can regard E_0 as shared entirely between electron and neutrino. Thus $qc = E_0 - E$. The number of states in phase space available to an electron, confined to a volume V with momentum $\boldsymbol{p} \to \boldsymbol{p} + d\boldsymbol{p}$ defined inside the element of solid angle $d\Omega$, is

$$\frac{V\, d\Omega}{h^3} p^2\, dp.$$

If the fermion wave functions are normalized to unit volume, $V = 1$, and we integrate over all space angles, the electron phase-space factor is

$$\frac{4\pi p^2\, dp}{h^3}.$$

Similarly, for the neutrino it is

$$\frac{4\pi q^2\, dq}{h^3}.$$

We disregard any possible correlation in angle between $\boldsymbol{p}$ and $\boldsymbol{q}$, and treat these two factors as independent, since the proton will take up the resultant momentum. [There is no phase-space factor for the proton since its momentum

is now fixed: $\boldsymbol{P} = -(\boldsymbol{p} + \boldsymbol{q})$.] So the number of final states is

$$d^2N = \frac{16\pi^2}{h^6} p^2 q^2 \, dp \, dq.$$

Also, for given values of p and E the neutrino momentum is fixed,

$$q = (E_0 - E)/c,$$

within the range $dq = dE_0/c$. Hence

$$\frac{dN}{dE_0} = \frac{16\pi^2}{h^6 c^3} p^2 (E_0 - E)^2 \, dp. \tag{4.2}$$

If $|M|^2$ is regarded as a constant, this last expression gives the electron spectrum

$$N(p)\, dp \propto p^2 (E_0 - E)^2 \, dp,$$

and thus if we plot $[N(p)/p^2]^{1/2}$ against E, a straight line cutting the x-axis at $E = E_0$ should result. This is called a *Kurie plot*. For many β-transitions, the Kurie plot is linear, as shown for the decay $H^3 \rightarrow He^3 + e^- + \bar{\nu}$ (mixed). In Fig. 4.3, $F(z, p)$ is a correction factor (~ 1 in this case) to account for the Coulomb effects on the electron wave function. For a nonzero neutrino mass, the plot bends over near the endpoint, and cuts the axis at $E' = E_0 - m_\nu c^2$. This particular decay, with small E_0, has been used to set an upper limit, $m_\nu < 60$ eV.

The total decay rate is obtained by integrating (4.2) over the electron spectrum. As a very crude approximation in some decays we can consider the

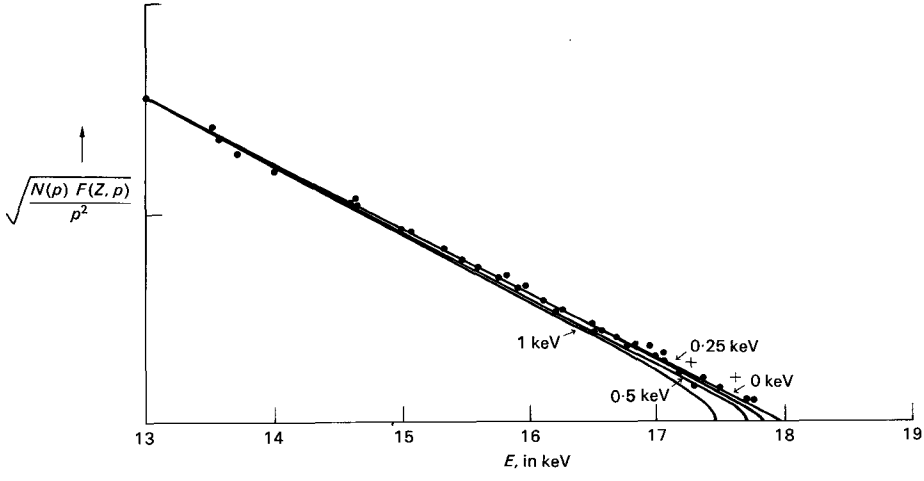

Fig. 4.3 Kurie plot for tritium β-decay. Deviations near the end point for various neutrino mass values are indicated. (After Langer and Moffat, 1952.)

electrons as extreme relativistic, $E \approx pc$ (not for tritium!), whence we obtain

$$N \sim \int_0^{E_0} E^2(E_0 - E)^2 \, dE = E_0^5/30. \tag{4.3}$$

Under these conditions, the disintegration constant (i.e. the decay rate) varies as the fifth power of the disintegration energy (the Sargent rule).

More generally, and including the Coulomb term, the transition rate will be

$$W = |M|^2 G^2 \frac{4\pi^2}{h} \frac{16\pi^2}{h^6 c^3} \int_0^{p_{\max}} F(z, p) N(p) \, dp.$$

If p, E are expressed in units of the electron mass, $p = p^1 \times mc$ and $E = E^1 \times mc^2$, the integral becomes

$$m^5 c^7 \int_0^{p^1_{\max}} F(z, p^1) N(p^1) \, dp^1 = m^5 c^7 f, \tag{4.4}$$

where f is a dimensionless number depending on $p^1_{\max}$ and the daughter nuclear charge z. Then

$$W = |M|^2 G^2 \frac{64\pi^4 m^5 c^4}{h^7} f \text{ transitions/sec.}$$

If t denotes the half-life, $W = (\log_e 2)/t$ so that

$$ft = \frac{K}{|M|^2} \qquad \text{where} \qquad K = \frac{h^7 \log_e 2}{64 G^2 \pi^4 m^5 c^4}. \tag{4.5}$$

The quantity ft therefore gives information about the matrix element M, which depends on the overlap of the initial and final nuclear wave functions. For allowed transitions, where the overlap is essentially complete, $|M|^2 \approx 1$. One finds that the observed β-decays subdivide into two more or less distinct classes: those of $\log_{10} ft$ of 3 to 4, corresponding to the allowed transitions discussed so far—and those of much larger ft values, with $\log_{10} ft$ of order 10 to 20. The latter are called forbidden transitions, and clearly involve much smaller values of $|M|^2$. They correspond crudely speaking to processes where the "electron-neutrino radiation" carries off orbital angular momentum, $l > 0$. Since the neutrino and electron are relativistic, it is not strictly possible to speak separately of their spin and orbital angular momentum. Only the total angular momentum, J_{lepton}, is a good quantum number. However, a nonrelativistic picture will serve to orient us on magnitude. We note first that the matrix element M will contain the product of four wave functions, ψ_i and ψ_f of the initial and final nuclear states, and u_1 and u_2 of the leptons. If we neglect Coulomb interactions we can represent the u's by the nonrelativistic plane wave form

$$u = e^{i\mathbf{k}\cdot\mathbf{r}} = 1 + i\mathbf{k}\cdot\mathbf{r} + \frac{(i\mathbf{k}\cdot\mathbf{r})^2}{2!} + \cdots, \tag{4.6}$$

where $\hbar k$ is the lepton momentum, and r the space coordinate relative to the nuclear center. One recognizes (4.6) as the multipole expansion of a plane wave. In the interaction region $r \approx R_0 \simeq \hbar/m_\pi c$, while $\hbar k \approx m_e c$, since Q-values in β-decay are of order of MeV. Thus $kr \simeq m_e/m_\pi \simeq 10^{-2}$. So, for an allowed transition (S-wave) the first term of (4.6) dominates and the integral of the ψ's and u's over the interaction volume gives unity. However, for a forbidden transition, for example $l = 1$, the first term cannot contribute, and the lepton wave functions give a factor of order $(kr)^2 = 10^{-4}$. The integral over the nuclear wave functions $\psi_f^* \psi_i$ is also small, since a forbidden transition involves a change in the configuration of the nucleus, including a change in parity. Another consequence is that, for a forbidden transition, the electron spectrum has extra terms [like $(kr)^2$, and therefore p^2 in the above example], which means that in general the Kurie plot (4.2) will no longer be a straight line.

From (4.5), we may calculate G for a pure Fermi transition by taking the observed ft value of O^{14}-decay, 3100 $\pm$ 20 sec, and assuming $|M|^2 = 1$. (This value of ft is a mean of recent values and incorporates some corrections.) Actually, we need to double the value of ft since O^{14} is a C^{12}-core plus two protons, either of which can decay. Inserting the numerical constants in (4.5), one gets

$$G = 1.4 \times 10^{-49} \text{ erg cm}^3$$
$$= \frac{10^{-5}}{M_p^2} \qquad \text{in units } \hbar = c = 1. \tag{4.7}$$

We have purposely quoted G here to only one decimal place, since a small correction is required in a more refined theory (Section 4.8.2).

We may also compare the O^{14} pure Fermi transition rate with that of the neutron, which is mixed. Call C_F and C_{GT} the coefficients corresponding to the Fermi and Gamow-Teller couplings. The neutron decay rate is then proportional to $C_F^2 + 3C_{GT}^2$. The factor 3 enters because there are $(2J + 1)$ or three possible orientations for the total angular momentum $J = 1$ of the leptons in a Gamow-Teller transition. If we consider only the total event rate, the two contributions add in quadrature. For the O^{14} rate, for the reason stated above, we write $2C_F^2$. Then

$$\frac{(ft)_{O^{14}}}{(ft)_n} = \frac{3100 \pm 20 \text{ sec}}{1080 \pm 16 \text{ sec}} = \frac{C_F^2 + 3C_{GT}^2}{2C_F^2},$$

which yields

$$\lambda = \left| \frac{C_{GT}}{C_F} \right| = 1.25 \pm 0.02. \tag{4.8}$$

Thus if we define the constant G for Fermi transitions, then for the Gamow-Teller transitions it has the slightly larger value λG. Note that the sign of λ is not determined here (actually it is negative). It may also be pointed out that (4.8) involves radiative and other corrections for O^{14}-decay. These can be

avoided in experiments with polarized neutrons, which give an independent value of λ (see Section 4.4).

4.2.3 Parity Nonconservation in β-decay

In 1956 Lee and Yang suggested that the weak interactions did not conserve parity (invariance under spatial inversions). They were forced to this conclusion owing to the absence of any direct experimental evidence to the contrary, and because of the so-called "$\tau - \theta$ paradox." The K^+-meson decays in several modes, two of which are:

$$K_{\pi 3}: \quad K^+ \to \pi^+ + \pi^+ + \pi^- \qquad \text{(historically the } \tau\text{-decay)},$$

$$K_{\pi 2}: \quad K^+ \to \pi^+ + \pi^0 \qquad \text{(historically the } \theta\text{-decay)}.$$

Analysis of the $K_{\pi 3}$-decay showed that the three pions were in an S-state (the mean kinetic energy per pion is only 25 MeV). Thus the spin-parity of the 3π-state is 0^- (see Chapter 7). In the $K_{\pi 2}$-decay, since $J = 0$, the 2π-parity must be even, i.e. a 0^+-state. If parity were conserved in both processes, then the τ and θ must be different particles. Eventually it became clear that the same particle was responsible for the two decay modes, and thus parity was violated. Could this be the case for weak interactions generally? A large number of experiments were done, showing that Lee and Yang were right. It is instructive to trace some of the history of why it took 22 years (from 1934) to get this basic information. Immediately after Dirac produced his celebrated equation describing relativistic spin $\frac{1}{2}$ particles with mass, Weyl (1929) showed that *zero* mass spin $\frac{1}{2}$ particles would be described by two simpler, decoupled equations, before ever the neutrino was invented. The trouble was that Weyl's equations described left-handed (longitudinally polarized) particles and right-handed antiparticles, or vice versa, and thus violated the parity principle.† They were abandoned because of Pauli's alleged remark, "God could not be only weakly left-handed." The techniques of low temperature necessary to align radioactive nuclei and investigate the possibility of parity violation existed long before 1956, but no one troubled to look since the theorists assured them there was nothing to find; parity must be conserved (as indeed it was, in electromagnetic and strong interactions).

The first experiment, by Wu *et al.* (1957), employed a sample of Co^{60} at 0.01°K inside a solenoid. At this temperature a high proportion of Co^{60} nuclei are aligned. $Co^{60}(J = 5)$ decays to $Ni^{60*}(J = 4)$—a pure Gamow-Teller transition. The relative electron intensities along and against the field direction were measured. The degree of Co^{60} alignment could be determined from observations of the angular distribution of γ-rays from Ni^{60*}. The results were

† The Dirac and Weyl equations are discussed in Appendix B.

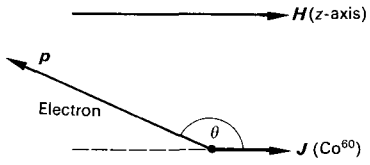

Figure 4.4

consistent with an intensity distribution of the form:

$$I(\theta) = 1 + \alpha \frac{(\boldsymbol{\sigma} \cdot \boldsymbol{p})}{E}$$

$$= 1 + \alpha \frac{v}{c} \cos \theta, \tag{4.9}$$

where $\alpha = -1$; $\boldsymbol{\sigma}$ = unit spin vector in direction $\boldsymbol{J}$; $\boldsymbol{p}$, E are the electron momentum and total energy; and θ is the angle of emission of the electron with respect to $\boldsymbol{J}$. The variation with electron velocity was checked over the range $0.4 < v/c < 0.8$.

The fore-aft asymmetry of $I(\theta)$ implies that the interaction violates parity conservation; for imagine the whole system reflected in a mirror normal to the z-axis. The first term (1) does not change sign under reflection—it is *scalar* (even parity). $\boldsymbol{\sigma}$, being an axial vector, does not change sign, while the polar vector $\boldsymbol{p} \rightarrow -\boldsymbol{p}$. Thus the product $\boldsymbol{\sigma} \cdot \boldsymbol{p} \rightarrow -\boldsymbol{\sigma} \cdot \boldsymbol{p}$ under reflection—it is called a *pseudoscalar* (odd parity). The fact that one has two such terms, of opposite parity, means that parity is not a well-defined quantum number in weak interactions. Note also that:

i) For a pure Fermi transition, $J_i = J_f = 0$, the nucleus could not be aligned and therefore parity violation could not be demonstrated by this method.

ii) Since $l = 0$ and $\Delta J = 1$ the spins of both electron and neutrino must be aligned along the positive z-axis. For $\theta = \pi$, when $I(\theta)$ is a maximum, the electron must then be left-handedly polarized.

This longitudinal polarization of electrons and positrons is found to be of the same form for Fermi, Gamow-Teller, and mixed transitions. If $\boldsymbol{\sigma}$ is the electron spin vector, the intensity is

$$I = 1 + \alpha \frac{\boldsymbol{\sigma} \cdot \boldsymbol{p}}{E}. \tag{4.10}$$

The polarization or *helicity* H is defined as

$$H = \frac{I_+ - I_-}{I_+ + I_-} = \alpha \frac{v}{c},$$

where I_+ and I_- represent intensities for $\boldsymbol{\sigma}$ parallel and antiparallel to $\boldsymbol{p}$.

Experimentally:

$$\alpha = +1 \text{ for } e^+, \qquad H = +\frac{v}{c},$$

$$= -1 \text{ for } e^-, \qquad H = -\frac{v}{c}. \tag{4.11}$$

The property of helicity is not limited to leptons. We have already seen that, owing to their zero mass, photons must be longitudinally spin polarized. There are right-handed (or right-circularly polarized) photons and left-handed photons, with helicities $+1$ and -1 respectively. Parity is conserved in electromagnetic processes involving photons, because the two types of photon are always emitted with equal probability, and one does not therefore observe a *net* circular polarization. On the contrary, in weak interactions, β-processes consist of the emission of *either* electrons with a net left-handed spin polarization, *or* positrons which are predominantly right-handed.

4.3 LEPTON POLARIZATION IN β-DECAY

4.3.1 Measurement of Electron Polarization

Experimentally, the longitudinal polarization of electrons has been observed by a variety of methods. Three of these are sketched diagrammatically in Fig. 4.5. In (a), the longitudinal polarization is turned into a transverse polariza-

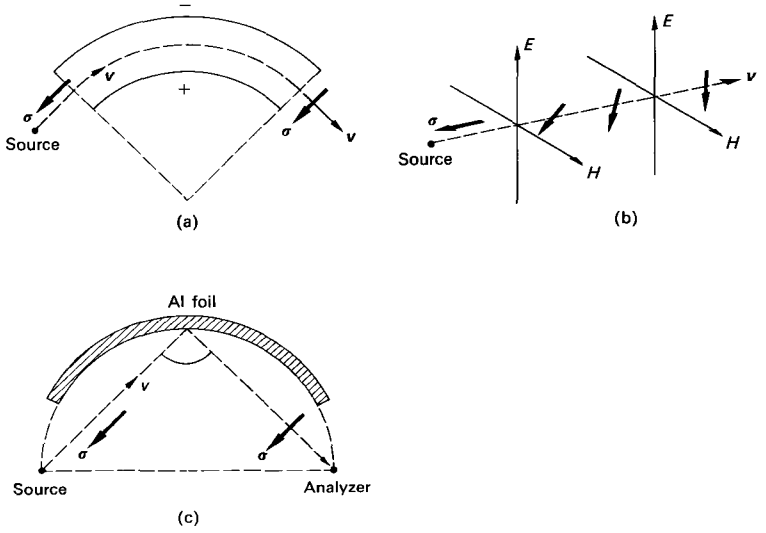

Fig. 4.5 Methods employed to transform longitudinal polarization of electrons from β-decay into transverse polarization. (a) Frauenfelder *et al.* (1957), (b) Cavanagh *et al.* (1957), (c) De Shalit *et al.* (1957).

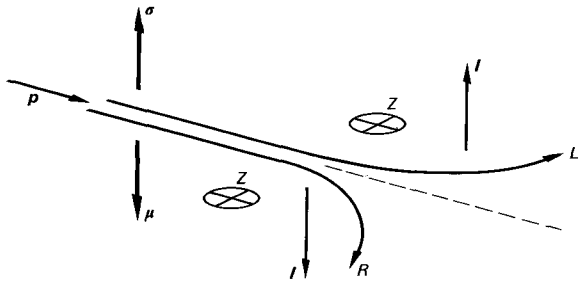

Fig. 4.6 Schematic diagram of scattering of a transversely polarized electron by a nucleus Z.

tion by electrostatic bending through 90°. Provided the electrons are non-relativistic ($v^2 \ll c^2$), the spin direction $\boldsymbol{\sigma}$ is virtually unaltered by the field (as $v \to c$, $\boldsymbol{\sigma}$ tends to follow the trajectory). A second technique, (b), employs crossed electric and magnetic fields. When $E/H = v/c$, the beam is undeflected, but $\boldsymbol{\sigma}$ precesses about $\boldsymbol{H}$. The value and extent of the fields is adjusted to give a 90° precession. A third method, (c), makes use of the fact that Coulomb scattering in a light element (in this case a 0.5-mm thick aluminum foil) does not affect the spin direction. The arrangement employs a semicircular strip of foil, with source and analyzer at each end of a diameter, resulting in a 90° scattering angle.

In each case the sense of polarization may be analyzed by observing the right-left asymmetry in the scattering by a foil of heavy element. The effect can be seen by a classical argument (Fig. 4.6). Let $\boldsymbol{l}$ be the orbital angular momentum of the electron relative to the scattering nucleus, Z. In the coordinate frame of the electron, the approaching nucleus appears as a positive current, clockwise or anticlockwise according to whether the electron passes to left or right. The magnetic field $\boldsymbol{H}$ associated with this current is therefore in the direction of $\boldsymbol{l}$. Let $\boldsymbol{\sigma}$ represent the spin vector of the electron; the spin magnetic moment $\boldsymbol{\mu}$ then points in the direction $-\boldsymbol{\sigma}$. It follows that the magnetic energy $\boldsymbol{\mu} \cdot \boldsymbol{H}$ is positive (i.e. one gets a repulsive force) when $\boldsymbol{l}$ and $\boldsymbol{\sigma}$ are parallel, and negative (attractive force) when $\boldsymbol{l}$ and $\boldsymbol{\sigma}$ are antiparallel. Thus the magnetic interaction arising from the spin-orbit coupling adds to the electrical force when $\boldsymbol{l} \cdot \boldsymbol{\sigma}$ is negative, and more electrons are scattered to right than to left. From the right-left asymmetry and a suitable calibration, the degree of transverse polarization can be determined.

The longitudinal polarization of electrons can also be found directly, without spin-twisting, by using a magnetized iron sheet and observing the electron-electron (Møller) scattering. Both electrons have to be observed in coincidence to distinguish the effect from the more intense nuclear scattering. The electron beam from the β-decay source falls obliquely on an iron foil

magnetized in its plane, so that $\boldsymbol{p}$ and $\boldsymbol{H}$ are parallel. The scattering is greatest when spins of incident and target electrons are parallel (i.e. $\boldsymbol{\sigma} \cdot \boldsymbol{H}/H = +1$). On reversing the field $\boldsymbol{H}$, the scattering ratio determines the longitudinal polarization. Another method is to observe the circular polarization of γ-rays from high energy bremsstrahlung when the electrons are stopped in an absorber. The sense of polarization of the forward γ-rays is the same as that initially possessed by the electrons, and is in turn determined by scattering in magnetized iron, as described below. Observations on the polarization of β-rays were carried out in numerous laboratories during 1957–58, and, within the experimental errors, clearly verified the helicity assignments (4.11).

4.3.2 Helicity of the Neutrino

The result (4.11), if applied to a neutrino ($m = 0$), implies that such a particle must be fully polarized, $H = +1$ or -1. In order to determine the type of operators occurring in the matrix element M in (4.1), the sign of the neutrino helicity turns out to be crucial. The neutrino is here defined as the neutral particle emitted together with the positron in β^+-decay, or following K-capture. The antineutrino then accompanies negative electrons in β^--decay. The neutrino helicity was determined in a classic and beautiful experiment by Goldhaber *et al.* in 1958. The steps in this experiment are indicated in Fig. 4.7.

i) Eu^{152} undergoes K-capture to an excited state of Sm^{152}, of $J = 1$, Fig. 4.7(a). In order to ensure conservation of angular momentum, $\boldsymbol{J}$ must be opposite to the spin of electron and neutrino. The recoiling Sm^{152}* therefore has the same sense of longitudinal polarization as the neutrino, Fig. 4.7(b).

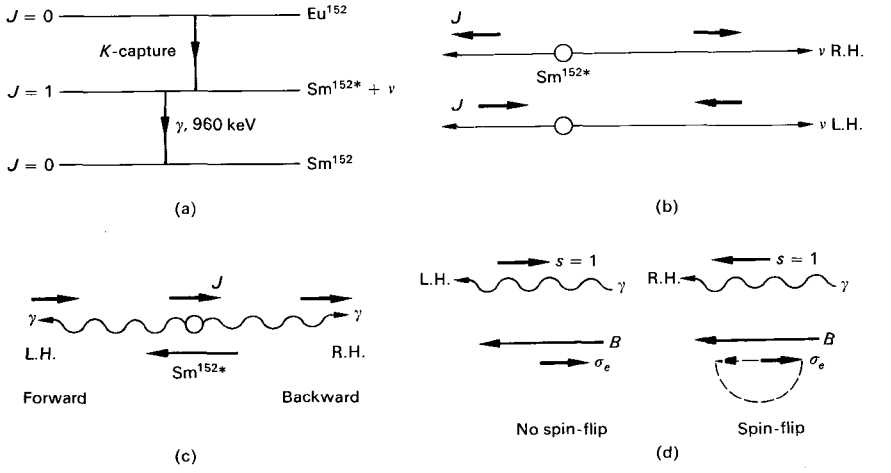

Fig. 4.7 Principal steps in the experiment of Goldhaber *et al.* to determine the neutrino helicity.

ii) Now, in the transition $Sm^{152*} \rightarrow Sm^{152} + \gamma$, γ-rays emitted in the forward (backward) direction with respect to the line of flight of Sm^{152*} will be polarized in the same (opposite) sense to the neutrino, as in Fig. 4.7(c). Thus, the polarization of the "forward" γ-rays is the same as that of the neutrino.

iii) The next step is to observe resonance scattering of the γ-rays in a Sm^{152} target. Resonance scattering is possible with γ-rays of just the right frequency to "hit" the excited state:

$$\gamma + Sm^{152} \rightarrow Sm^{152*} \rightarrow \gamma + Sm^{152}.$$

To produce resonance scattering, the γ-ray energy must slightly exceed the 960 keV to allow for the nuclear recoil. It is precisely the "forward" γ-rays, carrying with them a part of the neutrino-recoil momentum, which are able to do this, and which are therefore automatically selected by the resonance scattering.

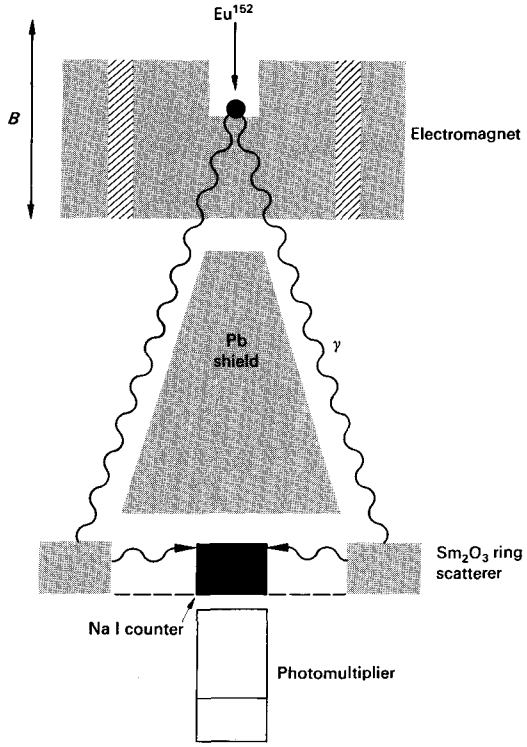

Fig. 4.8 Schematic diagram of apparatus used by Goldhaber *et al.* γ-rays from decay of Sm^{152*}, produced following K-capture in Eu^{152}, may undergo resonance scattering in Sm_2O_3, and are recorded by a sodium iodide scintillator and photomultiplier. The transmission of photons through the iron surrounding the Eu^{152} source depends on their helicity and the direction of the magnetic field B.

iv) The last step is to determine the polarization sense of the γ-rays. To do this, they were made to pass through magnetized iron before impinging on the Sm^{152} absorber. An electron in the iron with spin σ_e opposite to that of the photon can absorb the unit of angular momentum by spin-flip; if the spin is parallel it cannot. This is indicated in Fig. 4.7(d). If the γ-ray beam is in the same direction as the field $\boldsymbol{B}$, the transmission of the iron is greater for left-handed γ-rays than for right-handed.

A schematic diagram of the apparatus is shown in Fig. 4.8. By reversing $\boldsymbol{B}$ the sense of polarization could be determined from the change in counting rate. When allowance was made for various depolarizing effects, it was concluded that neutrinos were left-handedly spin polarized.

In conclusion, the helicity assignments for the leptons emitted in nuclear β-decay are therefore as follows:

Particle	e^+	e^-	ν	$\bar{\nu}$,
Helicity	$+v/c$	$-v/c$	-1	$+1$.

(4.12)

4.4 THE *V-A* INTERACTION

The formulas (4.9), (4.10), and (4.11) have been presented from a purely empirical viewpoint. In order to make theoretical predictions about β-decay, where we are concerned with relativistic particles of spin $\frac{1}{2}$, we should use the Dirac theory. This is described briefly in Appendix B; here we only outline the results which finally come out. In his original theory of β-decay, Fermi (1934) assumed that the matrix element of the interaction would involve a linear combination of the four fermion wave functions, and an appropriate operator O, say. (These wave functions are called spinors, each with four components.) Thus, for neutron decay, one could write, in obvious notation,

$$M = G(\psi_p^* O \psi_n)(\psi_e^* O \psi_\nu), \tag{4.13}$$

where G is the coupling constant typical of β-decay.

The grouping of the nucleon and the lepton wave functions in this way is made more plausible if we write the β-decay process

$$n \to p + e^- + \bar{\nu}$$

in the equivalent form

$$\nu + n \to p + e^-.$$

Fermi assumed an analogy between this process and the electromagnetic scattering of two charged particles, for example an electron and a proton:

$$e^- + p \to p + e^-.$$

The last process can be described as the interaction between two *currents:* an electron current $e(\psi_e^* O \psi_e)$ with a proton current $e(\psi_p^* O \psi_p)$. In the electromagnetic interaction, the operator O is a vector operator (actually $O = \gamma_4 \gamma_\mu$, where the γ's are 4×4 matrices, with index μ running from 1 to 4, which operate

on the 4-component spinor wave functions). Fermi assumed also that the operator O in (4.13) would again be a vector operator. The only differences from the electromagnetic case are that, for β-decay, one has a constant G instead of e^2; and that the "weak currents" in (4.13) are assumed to interact at a point, i.e. the weak interaction is of extremely short range. On the contrary, in the electromagnetic case, the interactions of the currents must be integrated over all space, since the Coulomb force is long-range. The current-current interaction is discussed further in Section 4.7.

The vector interaction was satisfactory (prior to the discovery of parity violation in 1956) in describing Fermi transitions. It did not account for Gamow-Teller transitions, since it could not produce a flip-over of the nucleon spin. Within certain requirements of relativistic invariance, one can in fact have five possible independent forms for the operator O in (4.13). They are called scalar (S), vector (V), tensor (T), axial vector (A), and pseudoscalar (P). These names are associated with the transformation properties of the weak currents under space inversions. The S- and V-interactions produce Fermi transitions, while T and A produce Gamow-Teller transitions. The pseudoscalar interaction P is unimportant in β-decay, since it couples spinor components proportional to particle velocity and thus introduces a factor in M^2 of v^2/c^2, where v is the nucleon velocity ($v^2/c^2 \sim 10^{-6}$ in β-decay).

The various operators O_i lead to different predictions on the angular correlations of the leptons in β-decay, and these are shown in Fig. 4.9. In these diagrams, v refers to the velocity of the positron.

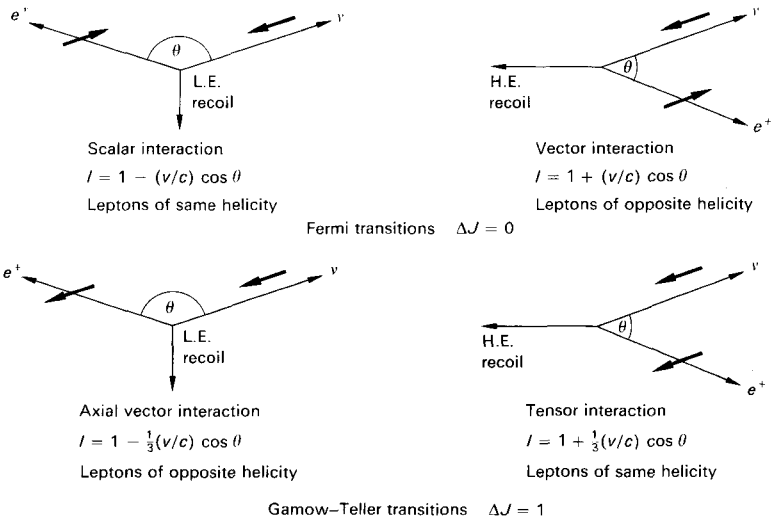

Fig. 4.9 Angular distributions in β-decay predicted by various types of interaction. The thick arrows denote lepton spin directions which result from angular momentum conservation assuming the neutrino is always left-handed. L.E. and H.E. represent low and high energy recoils respectively.

We note that, since in a Fermi transition the total angular momentum of the leptons is zero, the S-interaction must produce leptons of the same helicity, and the V-interaction, leptons of opposite helicity. In Gamow-Teller transitions, the total lepton angular momentum is $J = 1$, so that the T- and A-interactions produce leptons of the same and opposite helicities respectively. The foregoing experiments on lepton polarization, summarized in (4.12), show therefore that only the V- and A-interactions can produce the helicities actually observed. A similar conclusion is arrived at by studying the shape of the momentum spectra of the nuclear recoils in Fermi and Gamow-Teller transitions. We may also remark that the factor $\frac{1}{3}$ in the cos θ term for A- and T-couplings arises because the total angular momentum ($J = 1$) of the leptons possesses three possible orientations in space, and this reduces the angular correlation. Thus we can write in place of (4.13), for a general β-interaction,

$$M = G \sum_{i=V,A} C_i(\psi_p^* O_i \psi_n)(\psi_e^* O_i \psi_\nu), \tag{4.14}$$

where C_V and C_A are appropriate coefficients. For example, for a pure Fermi transition, $C_A = 0$. The matrix element (4.14) is, however, a scalar quantity. It implies that parity is conserved, and that, for each diagram in Fig. 4.9, we should add a second diagram with lepton spins reversed, so that there is no net lepton polarization. This is clearly wrong. We need to add another term to (4.14) which will give us a pseudoscalar quantity, so that the matrix element contains both scalars and pseudoscalars, and thus has no well-defined parity. We can do this simply by adding a similar expression, but with the operator in one bracket (the lepton bracket) multiplied by a matrix γ_5 ($\gamma_5 = \gamma_1\gamma_2\gamma_3\gamma_4$). Thus one obtains

$$M = G \sum_{i=V,A} (\psi_p^* O_i \psi_n)[\psi_e^* O_i (C_i + C_i' \gamma_5)\psi_\nu]. \tag{4.15}$$

If, as all the evidence suggests, the interaction is invariant under time reversal, it can be shown that C_i and C_i' must be real coefficients; furthermore, if a neutrino (or antineutrino) is to be completely spin polarized, $H = \pm 1$, one must have $C_i' = \pm C_i$. Since scalar and pseudoscalar terms then occur with equal magnitude, this is called the principle of *maximum parity violation*. For this case, the operator $(1 \pm \gamma_5)$ acting on the neutrino wave function in (4.15) projects out one sign of helicity:

$$(1 + \gamma_5) \rightarrow \text{L.H. neutrino state (R.H. antineutrino)},$$
$$(1 - \gamma_5) \rightarrow \text{R.H. neutrino state (L.H. antineutrino)}.$$

Since the experiment in Section 4.3.2 shows the neutrino to be left-handed, we need to take the first expression, corresponding to $C_i' = C_i$. This type of weak interaction is called the *two-component neutrino theory*, and was proposed independently by Lee and Yang, by Landau, and by Salam. It also correctly

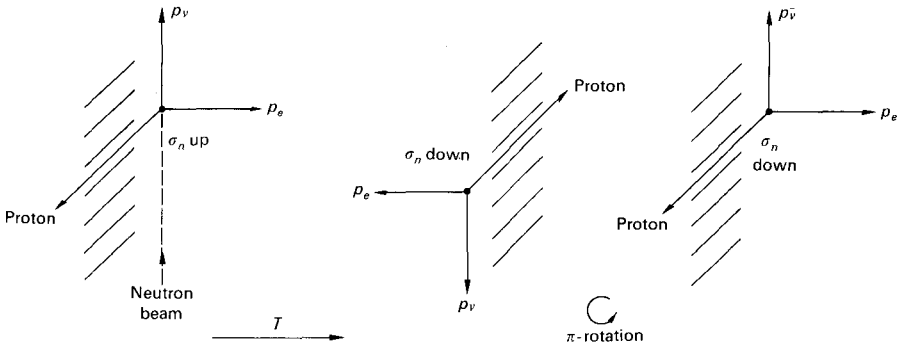

Fig. 4.10 Experiment to test time reversal invariance in polarized neutron decay. The electron and proton from neutron decay are detected in coincidence by counters to either side of the neutron beam. A slit system is used near the proton counter to ensure that the antineutrino travels preferentially in the neutron beam direction. The neutron spin $\boldsymbol{\sigma}_n$ is arranged normal to the beam and to the line joining the counters. Time reversal (see Table 3.6), followed by a 180° rotation of the figure, amounts to inversion of $\boldsymbol{\sigma}_n$ and therefore a change in sign of the D term in (4.17). If the decay is invariant under time reversal, D must be zero. This is investigated experimentally by reversing $\boldsymbol{\sigma}_n$ and observing the change in counting rate. (After Konopinski, 1959.)

predicts the helicities $\pm v/c$ for the charged leptons in (4.12). We may therefore rewrite (4.15) as

$$M = G \sum_{i=V,A} C_i(\psi_p^* O_i \psi_n)[\psi_e^* O_i(1 + \gamma_5)\psi_\nu]. \tag{4.16}$$

It remains to determine the ratio C_A/C_V and its sign. The sign can be determined by observing the interference terms between the V- and A-interactions in mixed transitions, and this has been accomplished by determination of angular correlations in the decay of *polarized* neutrons (in the decay of unpolarized neutrons, the V-A interference term is washed out in the sum over initial neutron spin). A classic series of experiments on polarized neutron decay have been carried out at Chalk River (1958), at the Argonne National Laboratory (1960, 1969), and in Moscow (1968). The principle of these experiments is to employ a polarized neutron beam (Section 3.18), to detect the proton and electron from neutron decay in coincidence, to either side of the neutron beam, and to vary the direction of neutron polarization relative to the counters in order to measure the various correlation coefficients in (4.17). The reader is referred to the review article by Konopinski (1959) for details. The measurement of the T-violating term D is illustrated in Fig. 4.10. Essentially the directions of three vectors may be determined experimentally; the neutron spin vector $\boldsymbol{\sigma}_n$ and the momentum vectors $\boldsymbol{p}$ and $\boldsymbol{q}$ of electron and antineutrino, the latter being deduced from observation of the recoil proton in the decay

$n \to p + e^- + \bar{\nu}$. The intensity or counting rate must then have the general form

$$I = 1 + a\left[\frac{\boldsymbol{q}\cdot\boldsymbol{p}}{qE}\right] + \left[A\frac{\boldsymbol{p}}{E} + B\frac{\boldsymbol{q}}{q}\right]\cdot\boldsymbol{\sigma}_n + D\left[\frac{\boldsymbol{p}\wedge\boldsymbol{q}}{qE}\right]\cdot\boldsymbol{\sigma}_n, \qquad (4.17)$$

where E is the total energy of the electron. The various coefficients a, A, B, and D are given by

$$\begin{aligned} a &= (C_V^2 - C_A^2)/(C_V^2 + 3C_A^2), && \text{(a)}\\ A &= [-2C_A^2 - (C_V C_A^* + C_V^* C_A)]/(C_V^2 + 3C_A^2), && \text{(b)}\\ B &= [+2C_A^2 - (C_V C_A^* + C_V^* C_A)]/(C_V^2 + 3C_A^2), && \text{(c)}\\ D &= i(C_V C_A^* - C_V^* C_A)/(C_V^2 + 3C_A^2), && \text{(d)} \end{aligned} \qquad (4.18)$$

where for generality we assume the coefficients C are complex numbers. As indicated from Table 3.6 and Fig. 4.10, the D term is the only one in (4.17) which changes sign under time reversal, and we see from (4.18d) that the D term must be zero (i.e. the interaction is T-invariant) if C_A and C_V are relatively real. Experimentally, it is found that D is consistent with zero, i.e.

$$C_A = |C_A/C_V| \times C_V e^{i\phi}$$

where $\phi = 0°$ or $180°$. Thus, $C_A \approx \pm C_V$. For these two possibilities, the values of A and B expected from (4.18), together with the observed values, are given in Table 4.1.

TABLE 4.1 Correlation coefficients in polarized neutron decay

	$C_A = +C_V$	$C_A = -C_V$	Experimental value
a	0	0	-0.1 ± 0.1[a]
A	-1	0	-0.11 ± 0.02[b] -0.115 ± 0.008[c]
B	0	$+1$	$+0.88 \pm 0.15$[b] $+1.01 \pm 0.04$[c]
D	0 (for T-invariance)		-0.04 ± 0.07[b] $+0.01 \pm 0.01$[d]

[a] Robson, *Phys. Rev.* **100,** 933 (1955).

[b] Burgy, Krohn, Novey, Ringo, and Telegdi, *Phys. Rev.* **120,** 1829 (1960).

[c] Christensen, Krohn, and Ringo, *Phys. Lett.* **28B,** 411 (1969).

[d] Erozolimsky, Bonlarenko, Mostovoy, Obinyakov, Zacharova, and Titov, *Phys. Lett.* **27B,** 557 (1968).

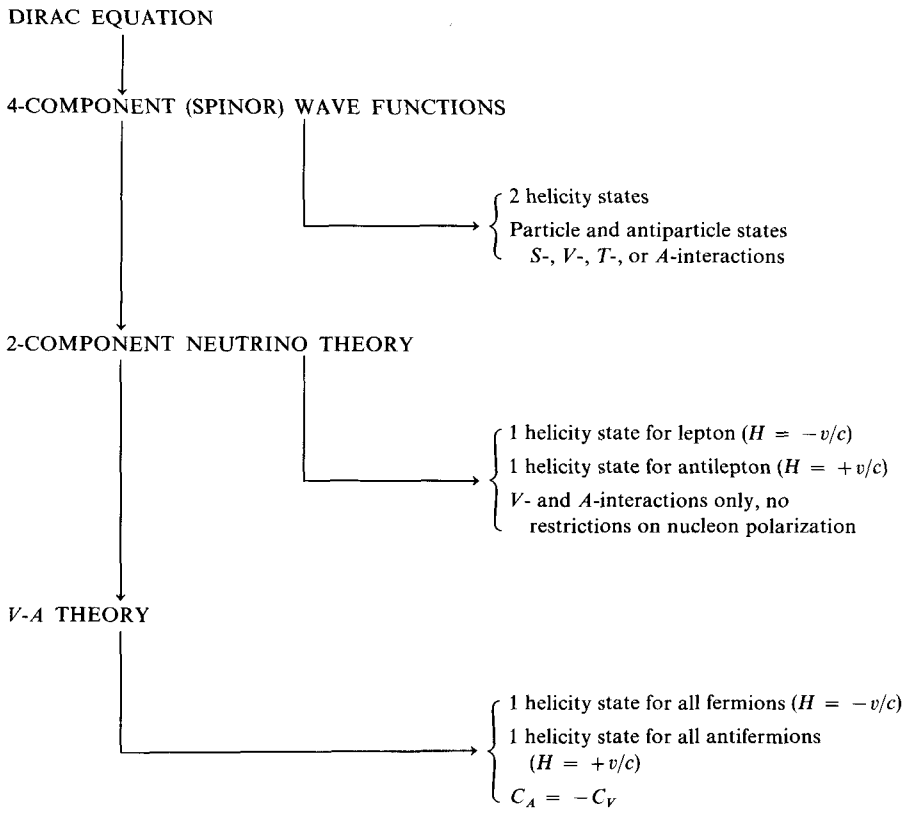

These results show clearly that C_A and C_V are of opposite sign. This is expressed briefly by saying that the interaction is $V - A$. The departures of A and B from 0 and 1 are accounted for by the fact that C_A and C_V, as we already know, are not quite equal. The values of C_A/C_V from (4.8) and from the experiment on polarized neutron decay are:

$$\begin{array}{lc} & \underline{C_A/C_V} \\ ft \text{ value of } O^{14} \text{ and neutron} & \pm(1.25 \pm 0.02), \\ \text{Polarized neutron decay} & -1.26 \pm 0.02. \end{array} \tag{4.19}$$

The latter value is inherently more reliable since it does not depend on radiative and other corrections required to arrive at the ft value for O^{14}-decay.

If we set $C_A = -\lambda C_V$, the β-decay interaction (4.16) may be shown to assume the form (see Appendix B):

$$M = GC_V[\psi_p^* O_V(1 + \lambda\gamma_5)\psi_n][\psi_e^* O_V(1 + \gamma_5)\psi_\nu], \tag{4.20}$$

where $O_V = \gamma_4\gamma_\mu$. We then note that, in the fictitious situation $\lambda = 1$ (pure V-A theory), the operators in the lepton and nucleon brackets are identical. This means that *all* fermions in the β-decay would have helicity $H = -v/c$ and all antifermions would have helicity $H = +v/c$, where v is the fermion velocity. This situation then differs from that of the pure vector interaction originally proposed by Fermi, (4.13), only in the inclusion of the projection operator $(1 + \gamma_5)$ in all terms. It is surmised that the departure of actual β-decay from the predictions of the pure V-A theory of Feynman and Gell-Mann (1958) and Marshak and Sudarshan (1958), is brought about by the effects of redistribution of the "weak charge" of the nucleon arising from the strong interactions; we explore this point in more detail later. In summary, the steps in the argument leading from the Dirac to the V-A theory are outlined in the flow diagram on p. 146.

4.5 PARITY VIOLATION IN Λ-DECAY

Parity nonconservation is a general property of weak interactions not solely associated with leptonic processes. The "τ-θ paradox," associated with the nonleptonic decay of kaons into pions, has already been mentioned. Another nonleptonic decay is that of the Λ-hyperon, for which the dominant decay modes are

$$\Lambda \to \pi^- + p, \qquad \Lambda \to \pi^\circ + n. \tag{4.21}$$

The Λ-hyperon does in fact also undergo leptonic β-decay, $\Lambda \to p + e^- + \bar{\nu}$, with a small branching ratio.

Parity violation can be demonstrated by considering the decay of Λ-hyperons produced in the associated production process

$$\pi^- + p \to \Lambda + K^\circ. \tag{4.22}$$

In this process, the Λ can be (and in general is) spin polarized. Parity conservation in such a strong interaction implies that the Λ must be polarized with spin $\boldsymbol{\sigma}$ *transverse* to the production plane, i.e. of the form $\boldsymbol{\sigma} \propto (\boldsymbol{p}_\Lambda \wedge \boldsymbol{p}_K)$, which does not change sign under inversion (Fig. 4.11). Note that spin polarization *in* the production plane in general does change sign, and is not allowed.

In practice the mean transverse polarization

$$P_\Lambda = (N\uparrow - N\downarrow)/(N\uparrow + N\downarrow) \approx 0.7$$

for an incident pion momentum in (4.22) just above 1 GeV/c. In the decay process (4.21), let us define the direction of $\boldsymbol{\sigma}$ as the z-axis of the Λ rest frame (Fig. 4.12). In this frame, the distribution in angle of emission (θ, ϕ) of the pion or proton will depend on their orbital angular momentum, l.

Since $J_\Lambda = \frac{1}{2}$, $J_z = \pm\frac{1}{2}$, we can have either $l = 0$ (proton and Λ-spins parallel) or $l = 1$ (spins antiparallel). Thus, we generally expect a combination

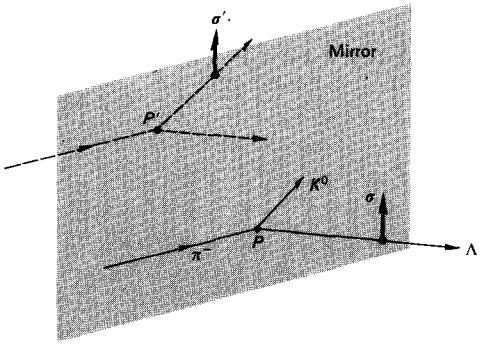

Fig. 4.11 Transverse polarization of the Λ-hyperon in the reaction $\pi^- + p \rightarrow \Lambda + K^0$ is invariant under spatial inversion, and therefore allowed for a strong reaction.

of s- and p-waves. Call m_1 the z-component of the proton spin vector, m_2 the z-component of $\boldsymbol{l}$. In the s-wave case, $m_2 = 0$ and the angular momentum wave function is $Y^l_m = Y^0_0$. Thus, for $J_z = +\frac{1}{2}$, the total wave function is the product

$$\psi_s = a_s Y^0_0 \chi^+, \tag{4.23}$$

where a_s denotes the s-wave amplitude and χ^+ the proton spin-up state of $m_1 = +\frac{1}{2}$. For the p-wave, $m_1 + m_2 = J_z = \frac{1}{2}$, with either $m_1 = +\frac{1}{2}$ and $m_2 = 0$, or $m_1 = -\frac{1}{2}$ and $m_2 = +1$.

Referring to Table 3.4, p. 101, for the Clebsch-Gordan coefficients for adding $J = 1$ and $J = \frac{1}{2}$, the entry for $J_{\text{total}} = m = +\frac{1}{2}$ gives

$$\psi_p = a_p[\sqrt{\tfrac{2}{3}} Y^1_1 \chi^- - \sqrt{\tfrac{1}{3}} Y^0_1 \chi^+]. \tag{4.24}$$

Here, a_s and a_p are, in general, complex amplitudes. Thus if *both* s- and p-waves

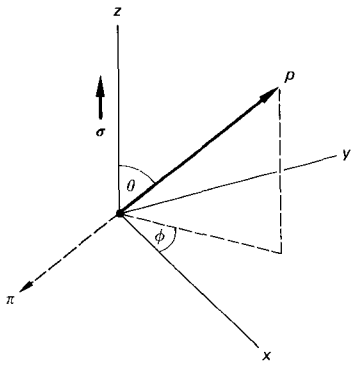

Fig. 4.12 Definition of axes and directions in Λ-decay.

are present, the total amplitude will be

$$\psi = \psi_s + \psi_p = \left[a_s Y_0^0 - \frac{a_p}{\sqrt{3}} Y_1^0\right]\chi^+ + [a_p\sqrt{\tfrac{2}{3}}Y_1^1]\chi^-.$$

Recalling the orthogonality of the spin states χ^+ and χ^-, the angular distribution becomes

$$\psi\psi^* = \left(a_s Y_0^0 - \frac{a_p}{\sqrt{3}} Y_1^0\right)\left(a_s Y_0^0 - \frac{a_p^*}{\sqrt{3}} Y_1^0\right) + a_p^2(\sqrt{\tfrac{2}{3}}Y_1^1)^2,$$

where one of the phases must be arbitrary and we take a_s to be real. Also, $Y_0^0 = 1$, $Y_1^0/\sqrt{3} = \cos\theta$, $\sqrt{\frac{2}{3}}Y_1^1 = -\sin\theta$, so that

$$\begin{aligned}\psi\psi^* &= |a_s|^2 + |a_p|^2\cos^2\theta + |a_p|^2\sin^2\theta - a_s\cos\theta\,[a_p + a_p^*] \\ &= |a_s|^2 + |a_p|^2 - 2a_s\,\mathrm{Re}\,a_p^*\cos\theta. \qquad (4.25)\end{aligned}$$

Setting

$$\alpha = \frac{2a_s\,\mathrm{Re}\,a_p^*}{|a_s|^2 + |a_p|^2},$$

the angular distribution has the form

$$I(\theta) = 1 - \alpha\cos\theta. \qquad (4.26)$$

The angle θ is defined relative to $\boldsymbol{\sigma}$; physically, one can only measure relative to the normal to the production plane, so that if we redefine θ in this way, the above result becomes

$$I(\theta) = 1 - \alpha P\cos\theta,$$

where P is the average polarization; experiment shows that $\alpha P \approx -0.7$. Thus, the parity violation in the Λ-decay is manifested as an up-down asymmetry of the decay pion (or proton) relative to the production plane.

Note that (4.26) has the same form as (4.9); that the parity violation parameter α is finite only if *both* a_s and a_p are finite; and thus that the parity violation arises from interference of the s (even) and p (odd) waves.

4.6 PION AND MUON DECAY

The lepton helicities first observed in 1957 in nuclear β-decay were detected simultaneously in the decay of pions and muons. We recall that the pion and muon decay schemes are

$$\pi^+ \to \mu^+ + \nu, \qquad (4.27)$$

$$\mu^+ \to e^+ + \nu + \bar{\nu}. \qquad (4.28)$$

Since the pion has spin zero, the neutrino and muon must have antiparallel spin vectors, as shown in Fig. 4.13. If the neutrino has helicity $H = -1$, as in

Fig. 4.13 Sketches indicating sense of spin polarization in pion and muon decay.

β-decay, the μ^+ must have negative helicity. In the subsequent muon decay, the positron spectrum is peaked in the region of the maximum energy, so the most likely configuration is that shown—the positron having positive helicity. In fact, the positron spectrum has the shape indicated in Fig. 4.14. This was originally of interest from the point of view of the identity of the ν and $\bar{\nu}$. The two neutrinos cannot be identical, otherwise the Pauli Principle would forbid them to be in the same quantum state, and the positron spectrum would go to zero at $E_{\max}$. It turns out that although they are ν and $\bar{\nu}$ they are different kinds of neutrinos anyhow; one is ν_e and the other $\bar{\nu}_\mu$ (see below). In the experiments, positive pions decayed in flight and those decay muons projected in the forward direction—thus with negative helicity—were selected. These μ^+ were stopped in a carbon absorber and the e^+ angular distribution relative to the original muon line-of-flight was observed. This latter will be antiparallel to the muon spin-vector, if there is no depolarization of the muons in coming to rest (true in carbon). The angular distribution observed was of the form

$$\frac{dN}{d\Omega} = 1 - \frac{\alpha}{3}\cos\theta, \tag{4.29}$$

where θ is the angle between $\boldsymbol{p}_\mu$, the initial muon momentum vector, and $\boldsymbol{p}_e$, the electron momentum vector, and $\alpha = 1$ within the errors of measurement. The same value of α was found for μ^+ and μ^-. Equation (4.29) is exactly the form predicted by the V-A theory. The helicity of the electrons (positrons) was also measured and shown to be $\mp v/c$.

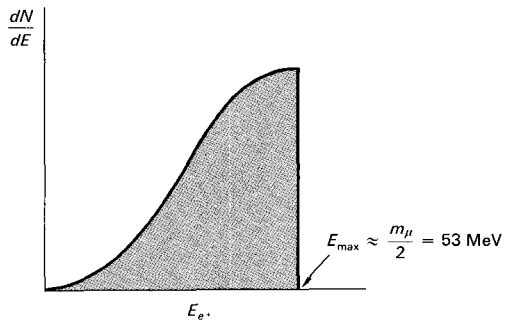

Fig. 4.14 Shape of positron energy spectrum from decay of positive muons (see also Fig. 4.16).

4.6.1 The $\pi \to \mu$ and $\pi \to e$ Branching Ratios

The decay (4.27) does not look like a 4-fermion interaction. However, if we imagine a nucleon-antinucleon intermediate state, we can draw the diagram of Fig. 4.15. It is difficult to calculate the matrix element directly—one obtains divergences when integrating over momentum in the intermediate $p\bar{n}$-state—but what we are interested in now is the ratio

$$\frac{\pi \to e + \nu}{\pi \to \mu + \nu}, \tag{4.30}$$

where everything to the left of the dotted line in Fig. 4.15 is common to both decays.

The π^+ has zero spin and odd parity, so that the virtual transition

$$\pi^+ \to p + \bar{n} \to e^+ + \nu; \qquad J^P = 0^-,$$

where nucleon and antinucleon have odd relative parity, may be thought of as the decay

$$p \to n + e^+ + \nu, \qquad \Delta J = 0, \text{ parity change.}$$

In the terminology of β-decay, the last reaction is a forbidden transition, in which the overall change in nuclear angular momentum is zero, resulting from spin-flip and the emission of the final nucleon in an orbital state $l = 1$—hence odd parity. Such a transition can only be produced by the axial vector (A) and pseudoscalar (P) couplings. There is no evidence for P-coupling in β-decay, but this might be ascribed to the very difficulty of generating a nucleon of $l = 1$ at the low energies available in such processes. Therefore, we must consider it as a possibility in the higher energy process of pion decay. As we have seen (Fig. 4.9), the A-coupling tends to produce leptons of opposite helicity. The P-coupling (not shown in Fig. 4.9) produces leptons of the same helicity. On the other hand, conservation of angular momentum compels the leptons to have the same helicity (Fig. 4.13). Thus, for A-coupling, we expect for the matrix element $M^2 \propto 1 + (-v/c)$—there being no factor $\frac{1}{3}$ here (as in Fig. 4.9) because we are considering a $\Delta J = 0$ transition instead of $\Delta J = 1$, with three projections of the lepton angular momentum in an arbitrary direction. For P-coupling, one finds instead $M^2 \propto (1 + v/c)$.

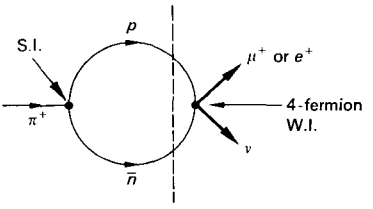

Fig. 4.15 The diagram for the decay $\pi^+ \to \mu^+ + \nu$, or $\pi^+ \to e^+ + \nu$, via a nucleon-antinucleon intermediate state.

The branching ratio (4.30) then follows if one includes the phase-space factor of (4.1). This is

$$\frac{dN}{dE_0} = \text{const. } p^2 \frac{dp}{dE_0}.$$

Here, $\boldsymbol{p}$ is the momentum of the charged lepton in the pion rest frame, v is its velocity and m its rest mass. The neutrino momentum is then $-\boldsymbol{p}$.

$-\boldsymbol{p}$ ← neutrino, $m = 0$ — m_π — charged lepton → $\boldsymbol{p}, m, v$

In units $c = 1$, the total energy is

$$E_0 = m_\pi = p + \sqrt{p^2 + m^2}.$$

Hence

$$\frac{dp}{dE_0} = \frac{(m_\pi^2 + m^2)}{2m_\pi^2},$$

$$1 + \frac{v}{c} = 2m_\pi^2/(m_\pi^2 + m^2),$$

$$1 - \frac{v}{c} = 2m^2/(m_\pi^2 + m^2).$$

Thus, for A-coupling the decay rate is given by

$$p^2 \frac{dp}{dE_0}\left(1 - \frac{v}{c}\right) = \frac{m^2}{4}\left(1 - \frac{m^2}{m_\pi^2}\right)^2,$$

and for P-coupling the decay rate is given by

$$p^2 \frac{dp}{dE_0}\left(1 + \frac{v}{c}\right) = \frac{m_\pi^2}{4}\left(1 - \frac{m^2}{m_\pi^2}\right)^2.$$

The predicted branching ratios become, with the approximation $m_e^2/m_\pi^2 \ll 1$,

A-coupling:
$$R = \frac{\pi \to e + \nu}{\pi \to \mu + \nu} = \frac{m_e^2}{m_\mu^2} \frac{1}{(1 - m_\mu^2/m_\pi^2)^2}$$
$$= 1.28 \times 10^{-4}, \tag{4.31a}$$

P-coupling:
$$R = \frac{\pi \to e + \nu}{\pi \to \mu + \nu} = \frac{1}{(1 - m_\mu^2/m_\pi^2)^2} = 5.5. \tag{4.31b}$$

The dramatic difference in the branching ratio for the two types of coupling just stems from the fact that angular momentum conservation compels the electron or muon to have the "wrong" helicity for A-coupling. The phase-space factor for the electron decay is greater than for muon decay, but the $(1 - v/c)$ term chops down hard on the more relativistic (i.e. lighter) lepton.

The first experiments to measure the ratio

$$R = \frac{\pi \to e + \nu}{\pi \to \mu + \nu}$$

in fact suggested a limit $R < 10^{-4}$. When Feynman and Gell-Mann put forward the V-A theory in 1958, they noted the discrepancy, and suggested that the early experiments were wrong. They were! The experiments were then repeated by several groups, and the results were consistent with the ratio 4.31(a).

The presently accepted experimental ratio is

$$R_{\text{exp}} = (1.25 \pm 0.03) \times 10^{-4}$$

compared with the V-A prediction, including radiative corrections, of

$$R_{\text{theor.}} = 1.23 \times 10^{-4}.$$

This result was a major triumph for the V-A theory, and proves that the pseudoscalar coupling is zero or extremely small. Figure 4.16 shows a typical electron spectrum observed from positive pions stopping in an absorber in one of the experiments. The rare $\pi \to e + \nu$ process yields electrons of unique energy, about 70 MeV. They are accompanied by the much more numerous electrons from the decay sequences $\pi \to \mu + \nu, \mu \to e + \nu + \bar{\nu}$. The spectrum

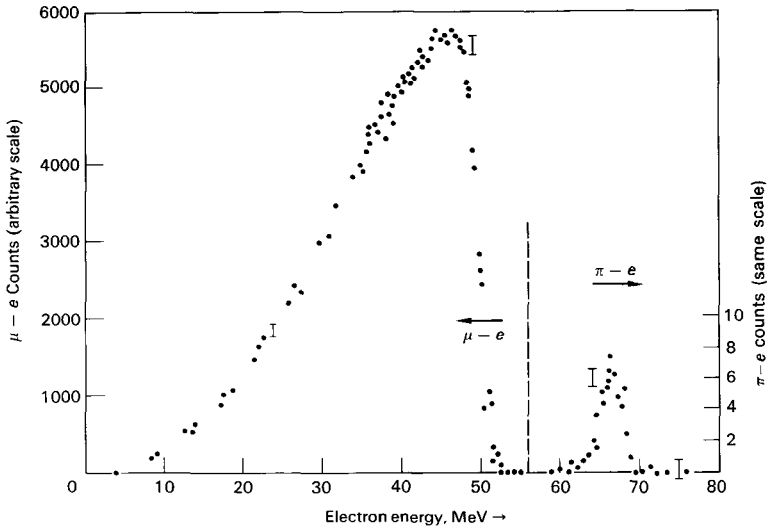

Fig. 4.16 Electron spectrum from stopping positive pions, as measured in the experiment of Anderson *et al.* (1960). The broad distribution extending up to 53 MeV is from $\mu^+ \to e^+ + \nu + \bar{\nu}$. The narrow peak around 70 MeV is from $\pi^+ \to e^+ + \nu$ decay. Note the change in vertical scale for these very rare events.

from the muon decay extends up to 53 MeV. The rejection of electrons from $\pi \to \mu \to e$ events is based on momentum, timing (the mean life of the pion being 2.5×10^{-8} sec, while that of the muon is 220×10^{-8} sec), and the absence of a muon pulse in the counters.

The formulas for R in (4.31) apply equally to the branching ratio

$$K \to e + \nu / K \to \mu + \nu,$$

if we use m_K in place of m_π. Since $m_K \sim 3m_\pi$, the electron is even more relativistic, and the ratio predicted for A-coupling is therefore smaller, $R = 2 \times 10^{-5}$. The average ratio from two recent experiments is $(2 \pm 0.5) \times 10^{-5}$, confirming the conclusions from pion decay.

4.7 THE CURRENT-CURRENT INTERACTION

4.7.1 Electron-Muon Universality, and Conservation of Vector Current

In deriving the branching ratios (4.31) in pion decay, we tacitly assumed equal weak couplings for the electron and muon decay modes. This hypothesis is known as *muon-electron universality*, and is clearly demonstrated in this case by the agreement between experiment and the prediction of the V-A theory.

Before enquiring further into what this means, let us look into electron-proton scattering, an electromagnetic interaction. We have already seen that it is convenient to consider this as an interaction between two electric currents via an intermediate virtual photon—see Fig. 4.17. Such a description is made possible essentially because fermions are conserved—two fermions in, two fermions out. In the scattering of two electrons *or* an electron and proton, we note that each of the currents carries the *same* unit of electric charge (e), and that this charge is conserved. This is not a trivial observation, as we shall see in discussing the case of weak currents. There is *prima facie* no reason why the proton and electron should have identical charges. Let us imagine that we can "turn off" the strong interactions. Then it is plausible to regard the proton as a "heavy electron" (like the muon). We would have a "bare" proton of charge e and magnetic moment equal to the Dirac value $eh/4\pi mc$. Now "turn on" the strong interactions. Then the proton immediately shows differences in behavior from the electron—for example, it develops a large anomalous magnetic moment. One can think of the strong interaction "structure" as being

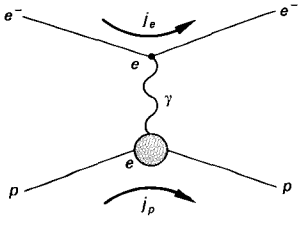

Fig. 4.17 The scattering of an electron by a proton, via an intermediary γ-ray, can be interpreted as an interaction between two currents, j_e and j_p.

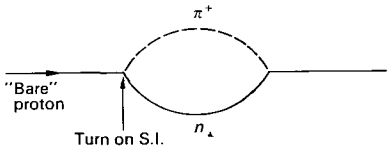

Figure 4.18

due to virtual emission and reabsorption of pions, or other particles, as in Fig. 4.18. Thus, although the *distribution* of electric charge is affected by the strong interactions, the *total* charge remains the same. In other words, the electromagnetic current j is conserved by the strong interactions.

Now consider the weak interaction. As indicated previously, we can again think of the β-decay process as an interaction of two currents. Figure 4.19 shows this for μ-decay. The current J carries a "weak charge," $\sqrt{G}$, instead of an electric charge, and there are three other important differences:

i) The weak currents are electric charge-changing ($n \to p$, $e^- \to \nu$) when they interact, so the intermediary particle W (if there is one) besides having unit spin like the photon, also carries an electric charge.

ii) Two weak currents interact effectively only at a *point* in space-time—as distinct from the electromagnetic case, where the interaction energy is obtained by integrating over all space, and as we know, many partial waves are involved.

iii) The electromagnetic interactions are pure vector, whereas the weak interactions are A and V, i.e. $J = J_A + J_V$.

The infinite range of the electromagnetic interaction is associated with the fact that the rest mass of the intermediary particle coupling the currents—the photon—is zero. The point-like interaction of the weak currents can be associated with the large mass of the intermediary boson W. At present (1971) this particle has not been observed experimentally, and its mass, if it exists, exceeds 2 GeV/c^2.

As we have drawn it, the weak charge, $\sqrt{G}$, of the muon and the electron are the same, and we have seen that this is verified experimentally by the $\pi \to e/\pi \to \mu$ branching ratio. At one time, it was thought that all elementary

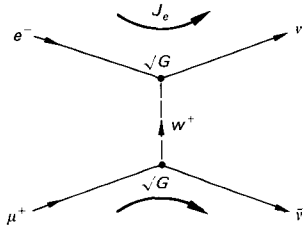

Figure 4.19

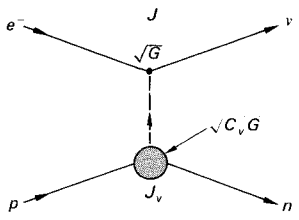

Figure 4.20

particles might have had the same unit of weak charge, just as they have the same electric charges—the so-called Universal Fermi Interaction (now dead).

Consider now the comparison between muon decay and a pure Fermi (V) nuclear transition, $O^{14} \rightarrow N^{14*} + e^+ + \nu$ (Fig. 4.20).

From the lifetime of these decays and the phase-space factors, one can compute the coupling constants involved. In muon decay it can be shown that the decay rate is $1/\tau_\mu = G^2 m_\mu^5/(192\pi^3)$, and inserting the observed lifetime gives the value of G (appropriate to muon decay):

$$G = \frac{1.02 \times 10^{-5}}{M_p^2}. \tag{4.32}$$

In O^{14}-decay, the ft value yields $G^2 C_V^2$, where C_V is an appropriate coefficient for vector β-decay. The experimental values yield

$$C_V = 0.98. \tag{4.33}$$

Thus the couplings in muon decay and in vector nucleon decay are very nearly (but not quite) the same. Let us for the moment neglect the 2% discrepancy. So the "vector weak charge" of the nucleon is unaffected by the strong interactions. Thus, the strong reaction properties of the nucleon, resulting in pion emission and reabsorption, $p \rightleftarrows n + \pi$, do not affect the "lepton-emitting power" of the nucleon; the vector weak current J_V is conserved by the strong interactions, just as is the electromagnetic current. This conclusion is called the *conserved vector current* (*CVC*) *hypothesis*.

One application of CVC is to the β-decay of the pion, Eq. (4.34). Consider the O^{14}-transition in the light of one of the possible virtual transitions of the nucleon, such as single pion emission. Part of the time, the proton exists in the state $(n + \pi^+)$; the neutron "core" cannot emit positron and neutrino, because of charge conservation, so that emission of leptons is entirely the responsibility of the π^+ and will be determined by the "weak charge" (vector part) of the pion. If this were not the same as that of the "bare" proton before the strong interactions were turned on, the result $C_V = 1.0$ would not hold. Thus the hypothesis also predicts that the coupling constants in the decays

$$\pi^+ \rightarrow \pi^0 + e^+ + \nu; \qquad J^P = 0^- \rightarrow J^P = 0^-; \qquad \text{pure Fermi} \tag{4.34a}$$

and

$$O^{14} \rightarrow N^{14*} + e^+ + \nu; \qquad J^P = 0^+ \rightarrow J^P = 0^+; \qquad \text{pure Fermi} \tag{4.34b}$$

should be the same, and hence they should have identical ft values (matrix elements). A very rough estimate of the decay rate (4.34) can be obtained by application of the Sargent rule (Eq. 4.3)—see Problem 4.2 at the end of the chapter. The observed branching ratio $(\pi^+ \to \pi^0 + e^+ + \nu)/(\pi^+ \to \mu^+ + \nu)$ is 1.02×10^{-8}, in perfect agreement with that expected from CVC.

4.7.2 Nonconservation of Axial Weak Current

As we know from (4.8) and (4.19), the axial vector current J_A is *not* conserved by the strong interactions, and the axial vector part of the weak charge of a nucleon is different from that of a lepton; $C_A = 1.25$. For a long time it has been speculated that the difference of C_A from unity—the divergence of

Figure 4.21

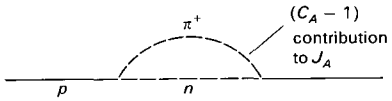

the axial current of the nucleon—is dominated by the process of single pion exchange. In other words, if the process of Fig. 4.21 did not exist, J_A would be a conserved current. Attempts have been made to calculate the magnitude of this term, and one gets good agreement with experiment (within $\sim 2\%$).

4.8 THE DECAYS OF STRANGE PARTICLES

4.8.1 Nonleptonic Decays; the $\Delta I = \frac{1}{2}$ Rule

Although weak interactions violate isospin conservation, there appears to be a selection rule

$$\Delta I = \tfrac{1}{2}$$

which is generally obeyed in the decays of strange particles (applying only to the nonleptonic decays, which have well-defined I-spin in the final state). The evidence for this rule comes, for example, from the branching ratios for Λ-decay:

$$\Lambda \to p + \pi^-$$
$$\to n + \pi^0.$$

Since $I_\Lambda = 0$, the $\Delta I = \frac{1}{2}$ rule states that the nucleon and pion must be in an $I = \frac{1}{2}$ state. Referring to the table of Clebsch-Gordan coefficients (p. 330) the rule predicts that

$$\frac{\text{Rate } \Lambda \to n\pi^0}{\text{Rate } \Lambda \to n\pi^0 + \text{Rate } \Lambda \to \pi^- p} = \frac{1}{3}. \tag{4.35}$$

The observed ratio is 0.36 ± 0.02, in excellent agreement with (4.35) when phase-space factors are included, which bring the expected value up to 0.345.

The reason for proposing the $\Delta I = \frac{1}{2}$ rule arose from a comparison of the decay modes of neutral and charged kaons to two pions:

	Decay rate	
$K^0 \to \pi^+ + \pi^-$	$7.7 \times 10^9\ \text{sec}^{-1}$,	(4.36a)
$K^+ \to \pi^+ + \pi^0$	$1.74 \times 10^7\ \text{sec}^{-1}$.	(4.36b)

The rate of reaction (4.36a) is about 400 times that of (4.36b). Since in each case the parent kaon has $J = 0$, then the boson pair has a symmetric space wave function, and hence a symmetric isospin wave function. The kaon has $I = \frac{1}{2}$, and the pair of pions has I integral and even (0 or 2). For the $\pi^+\pi^-$ state, we have $I_3 = 0$ and therefore $I = 0$ is allowed, whereas for the $\pi^+\pi^0$ state, $I_3 = 1$ and thus only $I = 2$ is possible. The $\Delta I = \frac{1}{2}$ rule thus allows (4.36a) and forbids (4.36b)—where one needs $\Delta I = \frac{3}{2}$ or $\frac{5}{2}$. The reason why $K^+ \to \pi^+ + \pi^0$ is allowed at all (if $\Delta I = \frac{1}{2}$ is valid), even if it is largely suppressed, is not clear at present.

4.8.2 Leptonic Decays: $\Delta Q = \Delta S$ Rule; Cabibbo Angle

For leptonic decays of strange particles, the isospin of the final state (containing leptons) cannot be specified, but empirically it appears that the rule $\Delta Q = \Delta S$ (i.e. the change in charge of hadron equal to the change in strangeness) is valid. From the relation (3.36),

$$Q = I_3 + \tfrac{1}{2}(B + S),$$

it follows that $\Delta I_3 = \frac{1}{2}$ if $\Delta Q = \Delta S = 1$.

As examples of the $\Delta Q = \Delta S$ rule, the decay

$$\Sigma^- \to n + e^- + \bar{\nu} \qquad (\Delta Q = \Delta S = +1)$$

is observed, but not

$$\Sigma^+ \to n + e^+ + \nu \qquad (\Delta S = +1, \Delta Q = -1).$$

Note that the process $\Delta Q = -\Delta S$ would allow $\Delta I_3 = \frac{3}{2}$ in the nonleptonic decays.

The Universal Fermi Interaction we mentioned earlier fails conspicuously when one considers the hyperon leptonic decay modes

$$\Lambda \to pe^-\bar{\nu}, \qquad \Sigma^- \to ne^-\bar{\nu}, \qquad \Xi^- \to \Lambda e^-\bar{\nu}.$$

The rates for these decays are roughly 20 times smaller than those expected if the couplings are the same as for the strangeness-conserving decays. Gell-Mann and Levy (1960) and Cabibbo (1963) proposed a way out of this difficulty. In the framework of unitary symmetry, dealt with in Chapter 6, the baryon states of spin-parity $\frac{1}{2}^+(n, p, \Sigma^+, \Sigma^-, \Sigma^0, \Lambda, \Xi^0, \Xi^-)$ form an octet. In the limit of exact symmetry, all these states would be degenerate, with identical masses and weak coupling. In nature the symmetry is broken, the eight states

being split according to the charge, or I_3, and the strangeness S. Thus the physical states n and p, with $S = 0$; Σ^+, Σ^-, Σ^0, and Λ, with $S = -1$; and Ξ^- and Ξ^0, with $S = -2$, have different masses. In this splitting, there is no *a priori* way to determine how the weak coupling is divided. Cabibbo postulated that for

$$\Delta S = 0 \text{ decays, weak coupling} = G \cos \theta,$$
$$\Delta S = 1 \text{ decays, weak coupling} = G \sin \theta.$$

Thus $J_{\text{hadronic}} = J_{(\Delta S=0)} \cos \theta + J_{(\Delta S=1)} \sin \theta$, where θ is an arbitrary angle, to be determined by experiment. Note that universality now appears by assigning the same coupling, G, to the leptonic current and to the hadronic current for the octet as a whole.

Thus, the coupling of the strangeness-conserving $n - p$ current (as in nuclear β-decay) to the lepton current would give a matrix element proportional to $G \cos \theta$; while in the decay $\Sigma^- \to ne^-\bar{\nu}$, the strangeness-changing $\Sigma^- - n$ weak current gives a matrix element proportional to $G \sin \theta$. The Cabibbo angle θ can be found by comparing observed $\Delta S = 0$ and $\Delta S = 1$ decay rates in unitary multiplets. For the decays of kaons and pions in the 0^- meson octet, one obtains for the amplitude ratios, when phase-space factors are divided out:

$$\left(\frac{K^+ \to \mu^+ + \nu}{\pi^+ \to \mu^+ + \nu}\right)_A \to \tan \theta_A = 0.275 \pm 0.003, \tag{4.37}$$

$$\left(\frac{K^+ \to \pi^0 + e^+ + \nu}{\pi^+ \to \pi^0 + e^+ + \nu}\right)_V \to \tan \theta_V = 0.251 \pm 0.008. \tag{4.38}$$

As we saw above, the decays (4.37) are axial-vector transitions, and hence are labeled A as involving axial currents, whereas those in (4.38) involve only vector weak currents and are labeled V. The fact that θ_A and θ_V are approximately equal was also predicted by the Cabibbo theory.

There are two important consequences of these results. First, the $\Delta S = 1$ baryonic decays are suppressed relative to the $\Delta S = 0$ decays. For example, the rate for $\Sigma^- \to n + e^- + \bar{\nu}$ is reduced relative to $n \to p + e^- + \bar{\nu}$ by a factor $\tan^2 \theta$, and this clears up the discrepancy noted above. Secondly, the coupling constant for Fermi transitions in β-decay becomes $G \cos \theta$ rather than G. If we define the vector weak coupling in β-decay as GC_V, as before, one obtains from (4.33) a value for the Cabibbo angle

$$\tan \theta = 0.22 \pm 0.02$$

in reasonable agreement with (4.38). Thus, the Cabibbo theory appears to account for most of the discrepancy between the Fermi constant value obtained from μ-decay and from β-decay. It is obvious that the Cabibbo angle is a

fundamental quantity, but why it has the particular value (4.38) is not at present clear.

4.9 CONSERVATION OF LEPTON NUMBER AND MUON NUMBER

According to the two-component neutrino hypothesis, neutrino and antineutrino are distinguished by having helicities of -1 and $+1$ respectively. If the mass of the neutrino is identically zero, this assignment is unique. (If the mass were finite, the neutrino velocity $v < c$, and it would be possible to transform into a frame with velocity exceeding v, in which the helicity would be reversed in sign.) Apart from the difference in helicity, the nonidentity of neutrino and antineutrino is also established from studies of the process of double β-decay. In favorable cases, it is possible for one nucleus to transform into another by the emission of two electrons and two antineutrinos, as a second order weak process:

$$Z \rightarrow (Z + 2) + 2e^- + 2\bar{\nu}. \tag{4.39}$$

However, if we regard neutrino and antineutrino as identical, we can imagine a two-step process:

$$Z \rightarrow (Z + 1) + e^- + \bar{\nu}\,(\equiv \nu),$$
$$\nu + (Z + 1) \rightarrow (Z + 2) + e^-,$$

or,

$$Z \rightarrow (Z + 2) + 2e^-, \tag{4.40}$$

in which the neutrino from the first step is absorbed in the second step. The result is neutrinoless double β-decay. Both (4.39) and (4.40) are second order processes. In (4.40), however, the disintegration energy is shared between two electrons only, and this process turns out to have a much shorter lifetime. Experiments indicate that (4.39) is the correct process, and thus that neutrino and antineutrino are not identical. For example, the observed lower limit to the lifetime for Ca^{48} double β-decay is 10^{19} yr, compared with theoretical estimates of $3 \times 10^{15\pm2}$ yr for the neutrinoless process (4.40), and $4 \times 10^{20\pm2}$ yr for (4.39). Another way of confirming this result was to show that the process

$$\bar{\nu} + Cl^{37} \rightarrow Ar^{37} + e^-$$

is not observed with antineutrinos from a reactor. If there had been no distinction between ν and $\bar{\nu}$, a measurable event rate would have been expected. As described in Section 1.3.2, these considerations are formalized by assigning the leptons e^-, μ^-, and ν a lepton number $L = +1$, and the antileptons e^+, μ^+, and $\bar{\nu}$ a lepton number $L = -1$, and postulating that the lepton number is absolutely conserved. Note that L is an additive quantum number.

The suspicion that there might be *two* types of neutrino (and antineutrino) associated with electrons and muons respectively, was aroused because certain

decays like

$$\mu^+ \to e^+ + \gamma,$$
$$\mu^+ \to e^+ + e^- + e^+$$

had never been observed, although no known selection rule forbade them. They could be forbidden, however, by postulating a conserved *muon number* as well as a lepton number:

$$\begin{aligned} & \mu^- \quad \nu_\mu \quad \mu^+ \quad \bar{\nu}_\mu \\ \text{Muon number} &= +1 \quad +1 \quad -1 \quad -1 \\ &= 0 \text{ for all other particles.} \end{aligned} \tag{4.41}$$

It is then necessary to distinguish between a neutrino ν_e accompanying an electron and one accompanying a muon, ν_μ. Examples are

$$\pi^+ \to \mu^+ + \nu_\mu,$$
$$n \to p + e^- + \bar{\nu}_e,$$
$$\mu^+ \to e^+ + \nu_e + \bar{\nu}_\mu.$$

In 1962/63 experiments at Brookhaven and CERN confirmed this hypothesis. A high energy (25 to 30 GeV) proton beam was used to produce pions from a target, which were focused by a magnetic "horn" and traversed a tunnel where a small fraction decayed. Neutrons and muons were removed by a thick (20-m) steel shield, leaving a beam of neutrinos (Fig. 4.22). The interactions of

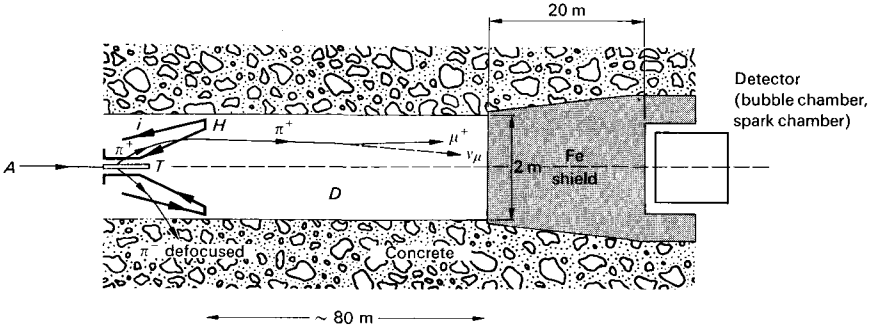

Fig. 4.22 Schematic diagram indicating principle of CERN high energy neutrino experiments (1963). A pencil proton beam *A* falls on a rod target *T*. Pion and kaon secondaries from the target are focused by means of a magnetic horn *H*. This consists of a conical sheet conductor through which flows a pulsed current of about 0.5 million A, thus producing an azimuthal magnetic field. Some 5% of the pions and kaons undergo decay in the tunnel *D*. Strongly interacting particles and muons are filtered out by a steel shield some 20-m thick. In later experiments, additional pulsed reflectors were included to enhance the neutrino flux. The decay tunnel length is about 80-m.

the type

$$\nu_\mu + n \rightarrow \mu^- + p \tag{4.42}$$

were observed, but not

$$\nu_\mu + n \rightarrow e^- + p. \tag{4.43}$$

A limit on the mass of ν_μ can be obtained from the kinematics of $\pi \rightarrow \mu + \nu_\mu$ and is currently $m_{\nu_\mu} < 1$ MeV (much poorer than the limit $m_{\nu_e} < 60$ eV, from tritium β-decay). This duality of electron and muon, and of electron and muon neutrino, is quite one of the most baffling of nature's extravaganzas.

Examples of high energy neutrino reactions in spark chambers and bubble chambers are given in Figs. 4.24, 4.25, and 4.26.

4.10 NEUTRINO INTERACTIONS

4.10.1 Reactor Experiments

Reactions like (4.42) are phenomenally difficult to observe on account of the very small cross section. The first observation of the interactions of free neutrinos was made by Reines and Cowan (1959). They employed a nuclear reactor as a source. Because uranium fission fragments are neutron-rich, they undergo radioactive β-decay, emitting negative electrons and antineutrinos. The flux of antineutrinos attainable is up to 10^{13} cm^{-2} sec^{-1}. Per fission, one obtains of order six antineutrinos, with a broad spectrum centered around 1 MeV. The reaction

$$\bar{\nu}_e + p \rightarrow n + e^+ \tag{4.44}$$

was observed, using a target of cadmium chloride ($CdCl_2$) and water. The positron produced in this reaction rapidly comes to rest by ionization loss, and forms positronium which annihilates to γ-rays, in turn producing fast electrons by Compton effect. The electrons are recorded in a liquid scintillation counter. The timescale for this process is of order 10^{-9} sec, so that the positron gives a so-called "prompt" pulse. The function of the cadmium is to capture the neutron after it has been moderated (i.e. reduced to thermal energy by successive elastic collisions with protons) in the water—a process which delays the γ-rays coming from eventual radiative capture of the neutron in cadmium, by several microseconds. Thus the signature of an event consists of two pulses microseconds apart. Figure 4.23 shows schematically the experimental arrangement. Two hundred litres of target are sandwiched in two layers between three tanks of liquid scintillator, which are viewed by banks of photomultipliers. Reines and Cowan observed a significant increase in comparing the coincidence rate with reactor on and off (the background in the experiment is attributed to cosmic rays). They also carried out various tests, such as diluting the water with heavy water, and proving that the rate varied as the normal water concentration (on account of the binding energy, the protons in the deuterium have a much smaller cross section).

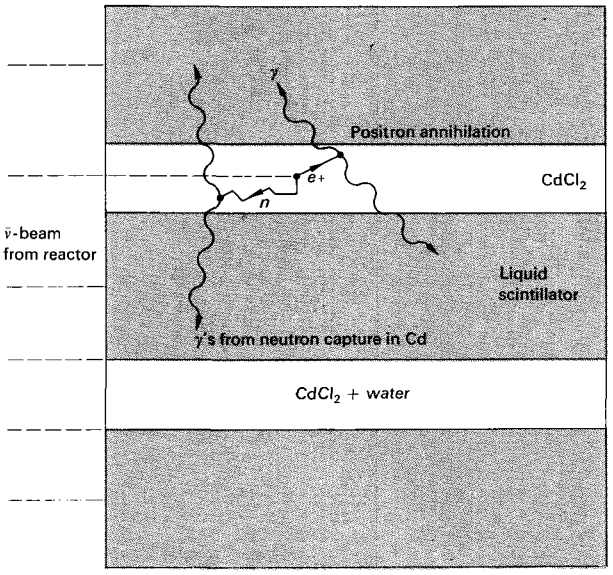

Fig. 4.23 Schematic diagram of the experiment by Reines and Cowan (1959), detecting the interactions of free antineutrinos from a reactor.

The expected magnitude of the cross section (4.44) is readily calculated. Using (3.16) for the transition rate, and integrating over solid angle, we have

$$W = \frac{2\pi}{\hbar}|M|^2 \frac{4\pi p^2\, dp}{h^3\, dE_0}.$$

From the relations

$$\sigma = \frac{W}{v_i}, \qquad \frac{dp}{dE_0} = \frac{1}{v_f},$$

it follows that

$$\sigma = \frac{1}{\pi\hbar^4}|M|^2 \frac{p^2}{v_i v_f},$$

where v_i and v_f are the relative velocities of the particles in the initial and final states, and $p_i = p_f = p$ is the numerical value of their momenta, all measured in the center-of-mass frame. In (4.44), the leptons are relativistic, while the nucleons have very low velocity. Thus $v_i \approx v_f \approx c$, and $pc \approx E$, the laboratory neutrino energy (the laboratory and center-of-mass reference frames are essentially one and the same). Setting $|M|^2 = (3C_A^2 + C_V^2)G^2 \approx 4G^2$, since we are dealing with a mixed transition, as in (4.8), and using natural units $\hbar = c = 1$, one obtains

$$\begin{aligned}\sigma &= \frac{4}{\pi}(GM_p)^2\left(\frac{p}{M_p}\right)^2; \qquad G = 10^{-5}/M_p^2 \\ &= \frac{10^{-10}}{M_p^2}\left(\frac{E}{M_p}\right)^2. \end{aligned} \tag{4.45}$$

Here, $1/M_p$ in the first term represents the proton Compton wavelength, $\lambda\!\!\!^{-}_p = 2 \times 10^{-14}$ cm. For $E = 1$ MeV, $(E/M_p) \approx 10^{-3}$, so that

$$\sigma \approx 10^{-44}\ \text{cm}^2. \tag{4.46}$$

The cross section observed by Reines and Cowan was consistent with this estimate. This cross section corresponds to a mean free path for antineutrinos in water of about 10^{21} cm or 1000 light years. We note that (4.45) predicts a cross section rising with phase-space, as the square of the center-of-mass momentum. This is a consequence of the s-wave nature of an allowed β-transition.

4.10.2 High Energy Experiments: Intermediate Boson

The reaction (4.42) typically involves neutrinos of energy about 1 GeV, thus $pc \approx 1$ GeV and $\sigma \sim 10^{-38}$ cm^2. Above 1 GeV neutrino energy, the cross section for (4.42) flattens off because of form-factor effects, associated with the "size" of the nucleon. Weak and electromagnetic form-factors are discussed in Chapter 5.

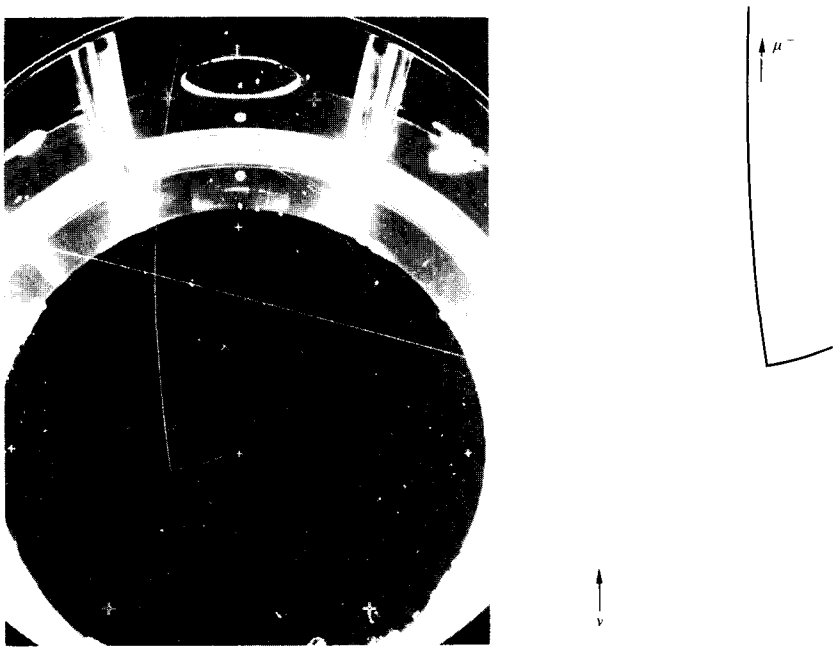

Fig. 4.24 Event attributed to an "elastic" neutrino interaction $\nu_\mu + n \to p + \mu^-$ in the CERN heavy liquid bubble chamber, filled with freon (CF_3Br). The negatively charged particle passes out of the chamber without interaction; it is attributed to a muon because, in many events of this type, the observed interaction length of the negative particles is very much larger than for strongly interacting particles. The original interaction takes place in a heavy nucleus, and one observes a proton plus a short nuclear fragment.

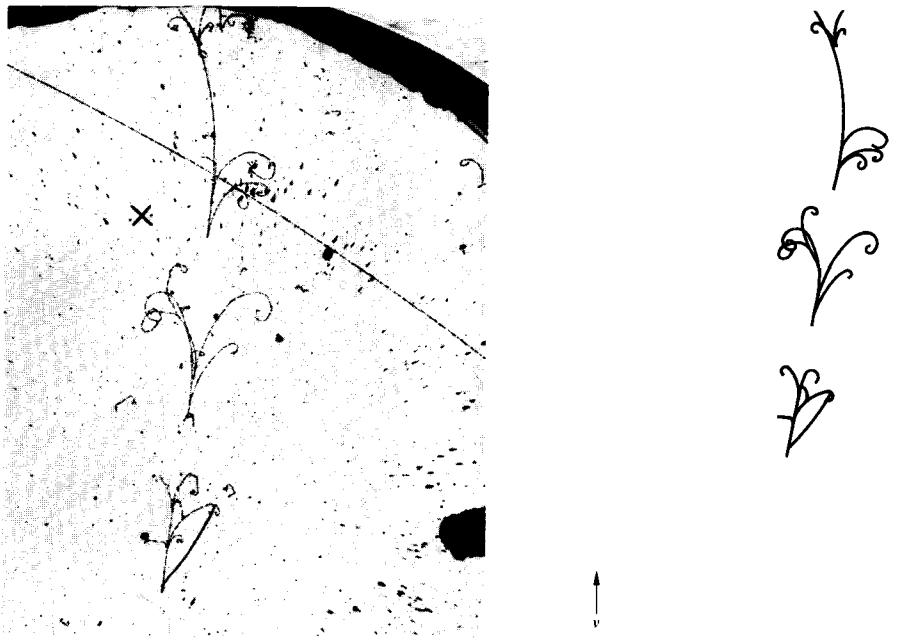

Fig. 4.25 Event produced by interaction of an electron-neutrino, ν_e: $\nu_e + n \rightarrow p + e^-$. The incident beam consists mostly of muon-neutrinos ν_μ, with a very small admixture of $\nu_e(\sim\frac{1}{2}\%)$ from the 3-body decays in flight, $K^+ \rightarrow \pi^0 + e^+ + \nu_e$. The high energy electron secondary is recognized by the characteristic shower it produces by the processes of bremsstrahlung and pair-production. The chamber diameter is 1.1 m, and the radiation length in CF_3Br is 0.11 m.

The relative numbers of events giving electron and muon secondaries is consistent with the calculated fluxes of ν_e and ν_μ in the beam, and thus confirms conservation of muon number. (Courtesy, CERN Information Service.)

A difficulty with the Fermi theory of the 4-fermion point interaction arises if we consider elastic scattering of neutrinos by electrons (not yet observed experimentally):

$$\nu_e + e^- \rightarrow e^- + \nu_e.$$

Here there are no form-factors, both particles being "point-like." Thus, even to the highest energies, the cross section has the form

$$\sigma_{\text{Fermi}} = \frac{4G^2}{\pi} p^2. \tag{4.47}$$

As before, p is the CMS momentum. A simple calculation gives $p^2 \simeq \frac{1}{2}m_e E$, so that the cross section rises linearly with the laboratory neutrino energy, E. On the other hand, the maximum value of the elastic scattering cross section,

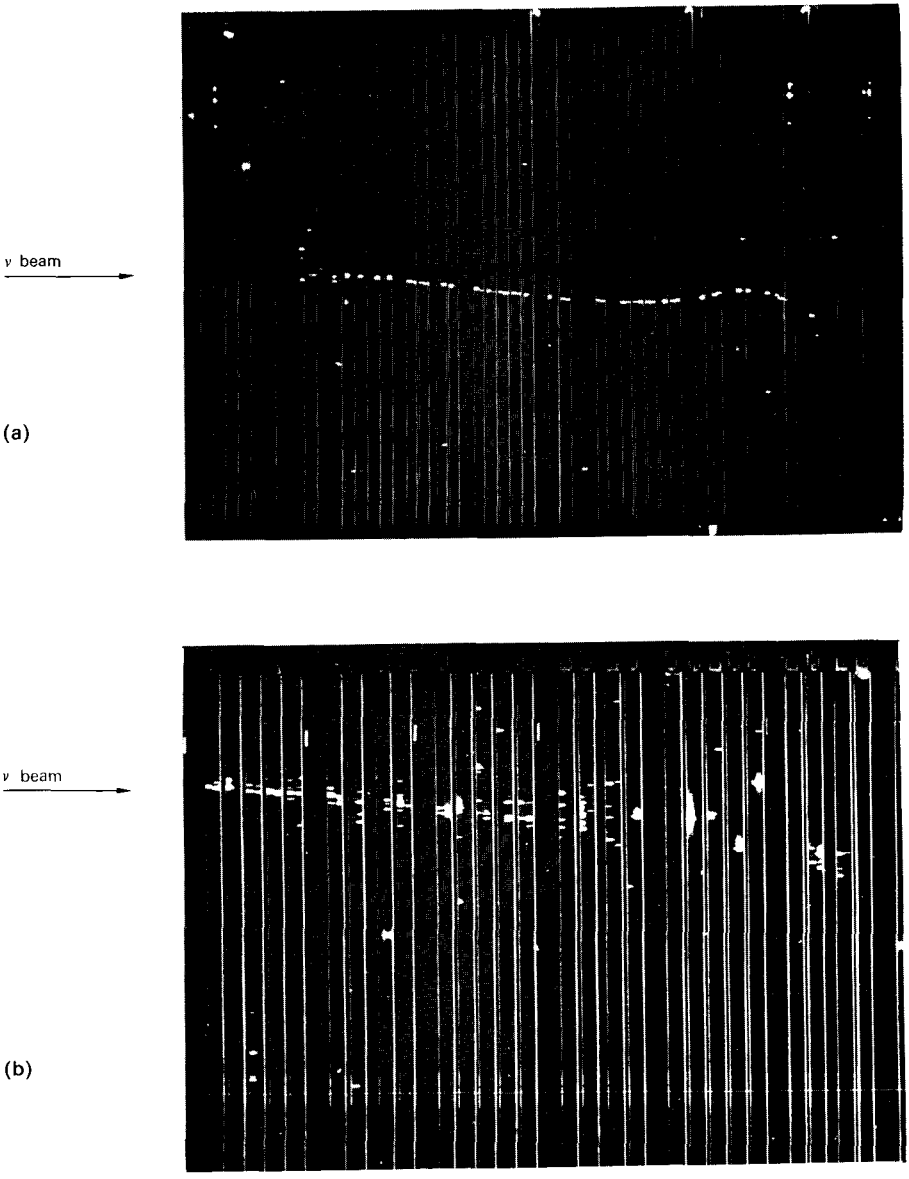

Fig. 4.26 (a) A neutrino event produced in CERN experiments employing a large spark chamber array, consisting of many plates of iron, brass, and aluminum. The muon track is characteristic, traversing many plates without interaction before coming to rest inside the chamber volume. (b) An event attributed to an electron neutrino, ν_e. The appearance of the scattered sparks due to the electron shower may be compared with the rectilinear muon track in event (a). (Courtesy, CERN Information Service.)

from ordinary wave theory, is (Section 7.2)

$$\sigma_{\max} = \pi \lambda\!\!\!^{-2} \sum_l (2l + 1), \tag{4.48}$$

where $\lambda\!\!\!^{-}$ is the de Broglie wavelength of the particles in the center-of-mass frame, and we sum over all partial waves of angular momentum l which contribute. For a point-like or s-wave interaction therefore, we obtain, in units $\hbar = c = 1$,

$$\sigma_{\max} = \frac{\pi}{p^2}.$$

Thus

$$\sigma_{\text{Fermi}} > \sigma_{\max}$$

when

$$p > G^{-1/2} \approx 300 M_p. \tag{4.49}$$

This means that, when the center-of-mass momentum exceeds about 300 GeV/c, the predicted cross section violates the wave theory limit, i.e. more particles are being scattered out into the final state than enter in the initial state. It is clear therefore that the Fermi theory is wrong in the limit of very high energy. One possible remedy is to "spread" the weak interaction from the point-like structure by postulating an intermediate spin 1 particle, the W-boson, coupling the (ν_e, e) and (e, ν_e) currents, as in Fig. 4.27(c). The effect of this would be to give $\sigma_{\max} \sim G^2 M_W^2$ and would solve this particular problem, provided $M_W < 300$ GeV. It may be remarked that the problem described above is not by any means the only thing wrong with the theory currently employed to describe the weak interactions, when one tries to extrapolate it to the high energy domain, or to convert it into a field theory like quantum electrodynamics. Such matters are, however, beyond the scope of this book.

In conclusion, we may summarize as follows: The original Fermi theory of the point interaction of four fermions has been suitably modified to account for parity violation (by including both axial and vector currents of opposite

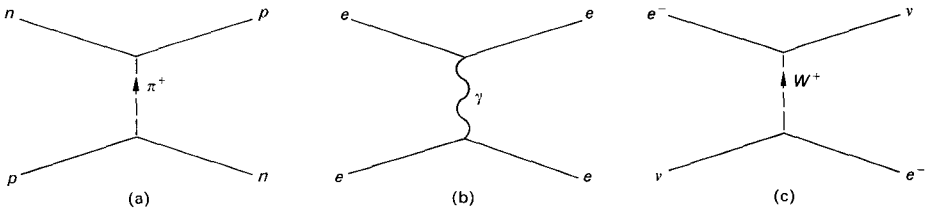

Fig. 4.27 Comparison of exchange mechanisms mediating the different types of interaction: (a) neutron-proton scattering mediated by pion exchange; (b) electron-electron (Møller) scattering via photon exchange; (c) neutrino-electron scattering via exchange of the proposed intermediate boson W of the weak interaction.

phase), and, by the Cabibbo prescription, to accommodate both strangeness-conserving and strangeness-violating processes. In this modified form it accounts very well indeed for a wide range of weak interaction processes.

4.11 K^0-DECAY

The strangeness scheme of Gell-Mann and Nishijima necessitates the introduction of two different neutral K-mesons, the K^0 with strangeness $S = +1$, and the $\overline{K^0}$ with strangeness $S = -1$. This follows from the assignment of isospin $\frac{1}{2}$ for the kaons (3.34) and the relation

$$\frac{Q}{e} = I_3 + \frac{S}{2} + \frac{B}{2}. \tag{4.50}$$

Thus the two kaon isospin doublets are

S \ I_3	$+\frac{1}{2}$	$-\frac{1}{2}$
$+1$	K^+	K^0
-1	$\overline{K^0}$	K^-

The K^0-particle can be produced in association with a hyperon or by charge exchange:

$$\begin{array}{cccccc} & \pi^- & + p & \rightarrow \Lambda & + K^0 & \\ S & 0 & 0 & -1 & +1, & \end{array} \tag{4.51}$$

$$\begin{array}{cccccc} & K^+ & + n & \rightarrow K^0 & + p & \\ S & +1 & 0 & +1 & 0, & \end{array} \tag{4.52}$$

while, since no $S = +1$ baryons appear to exist, $\overline{K^0}$ can be produced only by charge exchange, or in pairs with K^0 or K^+:

$$\begin{array}{cccccc} & K^- & + p & \rightarrow \overline{K^0} & + n & \\ S & -1 & 0 & -1 & 0, & \end{array} \tag{4.53}$$

$$\begin{array}{cccccc} & \pi^+ & + p & \rightarrow K^+ & + \overline{K^0} & + p \\ S & 0 & 0 & +1 & -1 & 0. \end{array} \tag{4.54}$$

We note that, using a pion beam, the threshold energy for (4.51) is less than for (4.54), so that it is experimentally simple to produce a pure K^0-source. K^0 and $\overline{K^0}$ are particle and antiparticle, and can be transformed one into the other by the operation of charge conjugation, which reverses the value of I_3 and the strangeness, S. As far as production in strong interactions is concerned, K^0 and $\overline{K^0}$ are eigenstates of the strangeness operator, with eigenvalues $+1$ and -1.

Neutral kaons are observed experimentally by their decay into other particles. Being the lightest strange particles, they can only decay weakly, into nonstrange particles, violating conservation of strangeness. For example, both K^0 and $\overline{K^0}$ can decay into two (or three) pions. The observation of such decays tells us nothing directly about whether the initial state was K^0 or $\overline{K^0}$—one has to look at the production mechanism (4.51) to (4.54) to decide that. The measured lifetime of the $\pi^+\pi^-$ decay mode is of order 10^{-10} sec and precisely the same for K^0 and $\overline{K^0}$. Fermi allegedly complained therefore that K^0 and $\overline{K^0}$ were really indistinguishable—simply figments of the imagination to fit the magic formula (4.50). The solution to this problem was provided by Gell-Mann and Pais (1955), with spectacular predictions. We first note that, since K^0 and $\overline{K^0}$ can *both* decay into two pions (or three pions), they can transform into one another via virtual intermediate pion states:

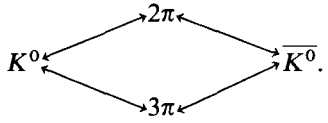

These virtual transitions involve $\Delta S = 2$, and thus are two-stage (or second order) weak interactions. Therefore, they are extremely weak, but nevertheless imply that, if one has a pure K^0-state at time $t = 0$, at any later time one will have a superposition of *both* K^0 and $\overline{K^0}$. This is a situation peculiar to neutral kaons. It does not happen for any other strange neutral particles, either because they decay by strong interactions ($\Delta S = 0$), if they are heavy enough, or because an absolute conservation rule forbids it. For example, the lambda and antilambda hyperon cannot "mix" because they have not only opposite strangeness, but opposite baryon number, and the latter is always conserved:

$$\begin{array}{cccccc} & \Lambda \to \pi^0 + n & & \pi^0 + \bar{n} \leftarrow \bar{\Lambda} \\ S & +1 \quad 0 & & 0 \quad -1 \\ B & +1 \quad +1 & & -1 \quad -1. \end{array}$$

The actual physical neutral kaon state observed at any finite distance from the source must therefore be written as

$$|K(t)\rangle = \alpha(t)\,|K^0\rangle + \beta(t)\,|\overline{K^0}\rangle.$$

The coefficients $\alpha(t)$ and $\beta(t)$ can be determined if we ask what are the eigenstates of the weak interaction responsible for the K^0-decay. In our discussion of weak interactions up to now, we have concluded that they are invariant under the CP-transformation, turning left-handed neutrinos into right-handed antineutrinos, and so on. Gell-Mann and Pais therefore argued that one should

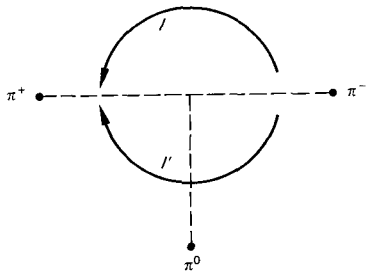

Figure 4.28

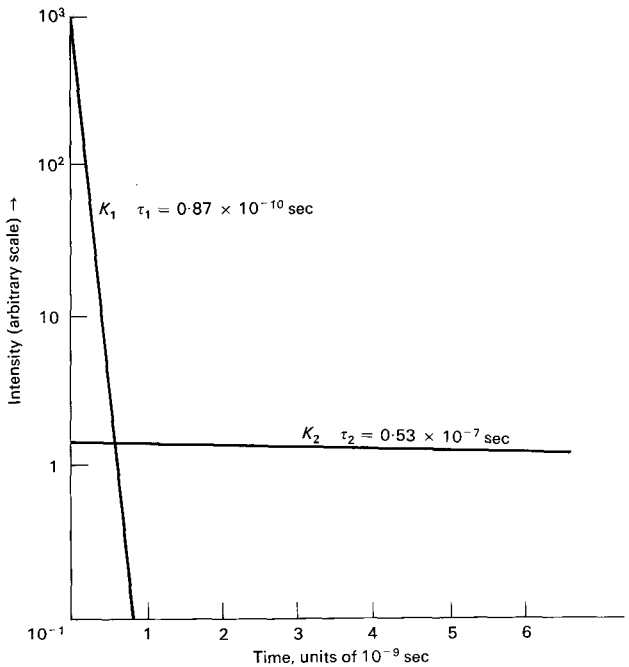

Fig. 4.29 Decay curves showing the components of a neutral kaon beam. The short-lived component K_1 decays to two pions, of *CP*-eigenvalue $+1$. The long-lived component K_2 has both nonleptonic and leptonic decay modes; the dominant pionic decay is to three pions, of *CP*-eigenvalue -1.

look for CP-eigenstates. If, in the K^0 rest frame, we consider CP acting on a K^0-state, this has the same effect as C alone, since the kaon has spin zero. Thus

$$\begin{aligned} CP\,|K^0\rangle &\to |\overline{K^0}\rangle, \\ CP\,|\overline{K^0}\rangle &\to |K^0\rangle. \end{aligned} \tag{4.55}$$

Clearly, $|K^0\rangle$ and $|\overline{K^0}\rangle$ are not CP-eigenstates. However, if we form the linear combinations

$$|K_1\rangle = \frac{1}{\sqrt{2}}(|K^0\rangle + |\overline{K^0}\rangle)$$

and

$$|K_2\rangle = \frac{1}{\sqrt{2}}(|K^0\rangle - |\overline{K^0}\rangle),$$

then

$$\begin{aligned} CP\,|K_1\rangle &\to \frac{1}{\sqrt{2}}(|\overline{K^0}\rangle + |K^0\rangle) = |K_1\rangle, \\ CP\,|K_2\rangle &\to \frac{1}{\sqrt{2}}(|\overline{K^0}\rangle - |K^0\rangle) = -|K_2\rangle. \end{aligned} \tag{4.56}$$

Thus $|K_1\rangle$ and $|K_2\rangle$ so defined are CP-eigenstates, with eigenvalues $+1$ and -1 respectively. We note that the relative phases of $|K^0\rangle$ and $|\overline{K^0}\rangle$ in (4.55) are arbitrary. $|K^0\rangle$ and $|\overline{K^0}\rangle$ are related by the C-operation, but we may always introduce an arbitrary phase factor, i.e. $C\,|K^0\rangle = e^{i\lambda}\,|\overline{K^0}\rangle$. This phase is, in principle, unobservable in the strong interactions, which cannot connect two states of different strangeness. The factor $1/\sqrt{2}$ in (4.56) is for normalization of the wave functions.

It is now apparent that, although $|K^0\rangle$ and $|\overline{K^0}\rangle$ could not be differentiated by their decay modes, the combinations $|K_1\rangle$ and $|K_2\rangle$ can. First consider a $2\pi^0$-state. This can only exist for $J = l$ even, since the neutral pions are spinless and indistinguishable, and the angular momentum wave function is therefore invariant under a 180° rotation which interchanges the two particles. Thus, the $2\pi^0$-state is even under both C and P and has CP-eigenvalue $+1$. For a $\pi^+\pi^-$-state, we must appeal to Bose symmetry. Since the total wave function, which consists of a product of a function of space coordinates and one of charge coordinates, is then symmetric under particle interchange, the eigenvalues of the C (charge interchange) operation and P (space inversion) operation must have the same sign, and hence the CP-parity is $+1$ again.

For a 3-pion state $\pi^+\pi^-\pi^0$, let us denote the total angular momentum as $\boldsymbol{J} = \boldsymbol{l} + \boldsymbol{l}'$ where $\boldsymbol{l}$ is the relative orbital angular momentum of the $\pi^+\pi^-$ combination, and $\boldsymbol{l}'$ is that of the π^0 with respect to the dipion (Fig. 4.28). Since the kaon has spin zero (Section 7.1.2) we must have $\boldsymbol{l} = -\boldsymbol{l}'$ and therefore $l = l'$. The simplest possibility is $l = l' = 0$. From the preceding argument,

the CP-parity of $\pi^+\pi^-$ is even. The π^0 has even C-parity, and space parity $P = (-1)(-1)^{l'} = -1$. Thus, the 3π-state of $l = l' = 0$ has CP-parity -1. For $l = l' = 1$, the CP-eigenvalue will be $+1$, but it can be shown that these modes are strongly inhibited by angular momentum barrier effects.

To summarize, therefore, and considering only the simplest 3π-state, the pion decay modes of the objects K_1 and K_2 will be:

$K_1 \to 2\pi$,	$CP = +1$,	high Q-value, therefore short lifetime ($\tau_1 = 0.87 \times 10^{-10}$ sec),
$K_2 \to 3\pi$,	$CP = -1$,	low Q-value, therefore long lifetime ($\tau_2 = 0.53 \times 10^{-7}$ sec).

The difference in lifetime is to be expected from the fact that the Q-value in the 2-pion decay (and hence the phase-space factor) is much greater than in the 3-pion decay (Fig. 4.29). The quoted lifetime τ_1 is the present value; actually it was known to be $\sim 10^{-10}$ sec from the early experiments, so that the Gell-Mann and Pais prediction was of a long-lived state K_2 of $\tau_2 \sim 10^{-7}$ sec. This was subsequently found in experiments at Brookhaven in 1956. Previously it had escaped discovery because K_2-decays would generally be a long way from the K^0-source; for example, a 1 GeV/c K_2-meson has a mean decay path of 30 m.

4.11.1 The K^0 Regeneration Phenomenon

The K_2 decay mode was not observed until some time after its prediction by Gell-Mann and Pais. However, Pais and Piccioni (1955) had observed that the $K_1 - K_2$ phenomenon would lead to the process of *regeneration*. Suppose we start with a pure K^0-beam, and let it coast *in vacuo* for the order of 100 K_1 mean lives, so that all the K_1-component has decayed and we are left with K_2 only. Now let the K_2-beam traverse a slab of material and interact. Immediately, the strong interactions will pick out the strangeness $+1$ and -1 components of the beam, i.e.

$$|K_2\rangle = \frac{1}{\sqrt{2}}(|K^0\rangle - |\overline{K^0}\rangle). \tag{4.57}$$

Thus, of the original K^0-beam intensity, 50% has disappeared by K_1-decay. The remainder, called K_2, upon traversing a slab where its nuclear interactions can be observed, should consist of 50% K^0 and 50% $\overline{K^0}$. The existence of $\overline{K^0}$ ($S = -1$) a long way from the source of an originally pure K^0-beam ($S = +1$) was confirmed by the observation of production of hyperons by Fry *et al.* in 1956. Thus $\overline{K^0} + p \to \Lambda + \pi^+$, for example.

The K^0- and $\overline{K^0}$-components in (4.57) must be absorbed differently; K^0-particles can only undergo elastic and charge exchange scattering, while $\overline{K^0}$-particles can also be absorbed in nuclear collisions, giving hyperons.

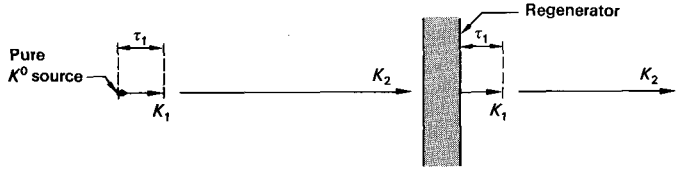

Fig. 4.30 Regeneration of short-lived K_1-mesons when a pure K_2-beam traverses a regenerator.

With more strong channels open, the $\overline{K^0}$ is therefore absorbed more strongly than K^0. After emerging from the slab, we shall therefore have a K^0-amplitude $f|K^0\rangle$ and a $\overline{K^0}$-amplitude $\bar{f}|\overline{K^0}\rangle$ say, where $\bar{f} < f < 1$. If we then ask what are the characteristics of the emergent beam with respect to decay, we must write, in place of (4.57):

$$\frac{1}{\sqrt{2}}(f|K^0\rangle - \bar{f}|\overline{K^0}\rangle) = \frac{(f+\bar{f})}{2\sqrt{2}}(|K^0\rangle - |\overline{K^0}\rangle) + \frac{(f-\bar{f})}{2\sqrt{2}}(|K^0\rangle + |\overline{K^0}\rangle)$$
$$= \tfrac{1}{2}(f+\bar{f})|K_2\rangle + \tfrac{1}{2}(f-\bar{f})|K_1\rangle. \qquad (4.58)$$

Since $f \neq \bar{f}$, it follows that some of the K_1-state has been regenerated (Fig. 4.30). This regeneration of short-lived K_1's in a long-lived K_2-beam was confirmed by experiment.

The regeneration phenomenon in K^0-decay, at first startling, is simply a consequence of the concepts of superposition and quantization in wave mechanics. The behavior of a proton or atomic beam in an inhomogeneous magnetic field provides a fairly close analogy. Referring to Fig. 4.31, suppose we have an initially unpolarized proton beam moving along the z-axis, which then traverses an inhomogeneous field H_y directed along the y-axis (representing the strong interaction in the K^0 case). The protons are then quantized in two spin eigenstates, $\sigma_y = +\frac{1}{2}$ and $\sigma_y = -\frac{1}{2}$, particles in the first state being deflected upward and those in the second downward. (These are analogous to the K^0 and $\overline{K^0}$ S-eigenstates.) We select the part of the beam deflected upward, and pass it through an inhomogeneous field along the x-axis, H_x (the analog of

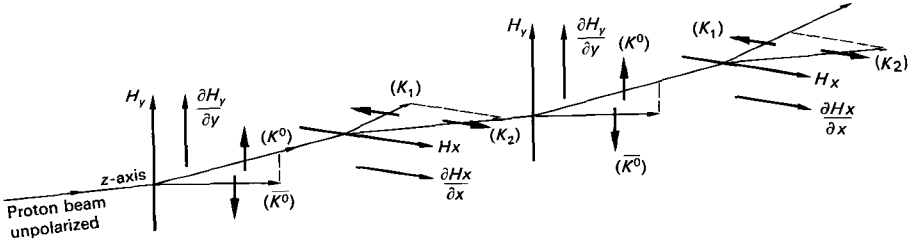

Fig. 4.31 Analogy between deflection of proton beam in two orthogonal planes, by means of inhomogeneous magnetic fields, and the K^0-decay and regeneration phenomena.

the weak interactions). The beam again splits into two components, 50% having $\sigma_x = -\frac{1}{2}$ and being deflected to the left, and 50% having $\sigma_x = +\frac{1}{2}$, deflected to the right. Note that *all* information about quantization along the y-axis has necessarily been lost. In turn, if we take the $\sigma_x = \frac{1}{2}$ component (corresponding to K_2), we may again pass it through a field along the y-axis, and recover the components $\sigma_y = \pm\frac{1}{2}$, and lose all knowledge of σ_x (analogous to regeneration of K^0 and $\overline{K^0}$ in an absorber). Finally, passage through a field H_x yields as eigenvalues $\sigma_x = \pm\frac{1}{2}$ (corresponding to reappearance of K_1). To make the analogy more exact, i.e. account for the different decay and nuclear absorption probabilities in the K^0 problem, one could arrange to absorb components of the proton beam deflected in two of the four directions.

The important feature of the Stern-Gerlach proton beam experiment is that it is impossible simultaneously to quantize the spin components of the beam along two orthogonal axes. This may also be stated by saying that the spin operators σ_x and σ_y do not commute; or, of the three matrix operators σ_x, σ_y, and σ_z, only one may be diagonalized at a time (i.e. possess only diagonal elements, and have real, nonzero eigenvalues). Since an operator with real eigenvalues must commute with the Hamiltonian (energy) operator, the axis singled out in space is necessarily that defined by the magnetic field. In a similar fashion, the *CP*- and *S*-operators do not commute, so that one can have states which are eigenstates of *CP or S*, but not both.

4.11.2 Strangeness Oscillations

So far, we have combined K_1- and K_2-amplitudes without regard to their precise time dependence, in order to bring out the main features of the regeneration phenomena in the simplest way. To be more specific we should include phase factors with the amplitudes. The relative phase of K_1- and K_2-states of a given momentum will only be constant with time if these particles have identical masses. K_1 and K_2 are not charge conjugate states, having quite different decay modes and lifetimes, so that, in the same sense that the mass difference between neutron and proton can be attributed to differences in their electromagnetic coupling, a $K_1 - K_2$ mass difference—but a very much smaller one—is to be expected because of their different weak couplings.

The amplitude of the state K_1 at time t can be written as

$$a_1(t) = a_1(0)e^{-(iE_1/\hbar)t} \times e^{-\Gamma_1 t/2\hbar}, \tag{4.59}$$

where E_1 is the total energy of the particle, so that $E_1/\hbar$ is the circular frequency, ω_1, and $\Gamma_1 = \hbar/\tau_1$ is the width of the state, τ_1 being the mean lifetime in the frame in which the energy E_1 is defined. The second term must have the form shown, in accord with the law of radioactive decay of the intensity:

$$\begin{aligned} I(t) &= a_1(t) \times a_1^*(t) = a_1(0)a_1^*(0)e^{-\Gamma_1 t/\hbar} \\ &= I(0)e^{-t/\tau_1}. \end{aligned}$$

Setting $\hbar = c = 1$ and measuring all times in the rest frame, so that τ_1 is the proper lifetime and $E_1 = m_1$, the particle rest mass, the K_1-amplitude is

$$a_1(t) = a_1(0)e^{-(\Gamma_1/2 + im_1)t}. \tag{4.60a}$$

Similarly, for K_2,

$$a_2(t) = a_2(0)e^{-(\Gamma_2/2 + im_2)t}. \tag{4.60b}$$

Now suppose that at $t = 0$, a beam of unit intensity consists of pure K^0. Then $a_1(0) = a_2(0) = 1/\sqrt{2}$. After a time t for free decay *in vacuo*, the K^0-intensity will be

$$\begin{aligned} I(K^0) &= \frac{[a_1(t) + a_2(t)]}{\sqrt{2}} \frac{[a_1^*(t) + a_2^*(t)]}{\sqrt{2}} \\ &= \tfrac{1}{4}[e^{-\Gamma_1 t} + e^{-\Gamma_2 t} + 2e^{-[(\Gamma_1 + \Gamma_2)/2]t} \cos \Delta m t], \end{aligned} \tag{4.61}$$

where $\Delta m = |m_2 - m_1|$. Similarly, the $\overline{K^0}$-intensity will be, writing the amplitude as $[a_1(t) - a_2(t)]/\sqrt{2}$,

$$I(\overline{K^0}) = \tfrac{1}{4}[e^{-\Gamma_1 t} + e^{-\Gamma_2 t} - 2e^{-[(\Gamma_1 + \Gamma_2)/2]t} \cos \Delta m t]. \tag{4.62}$$

Thus, the K^0- and $\overline{K^0}$-intensities *oscillate* with the frequency Δm. Figure 4.32 shows the variation to be expected for $\Delta m = 0.5/\tau_1$. If one measures the

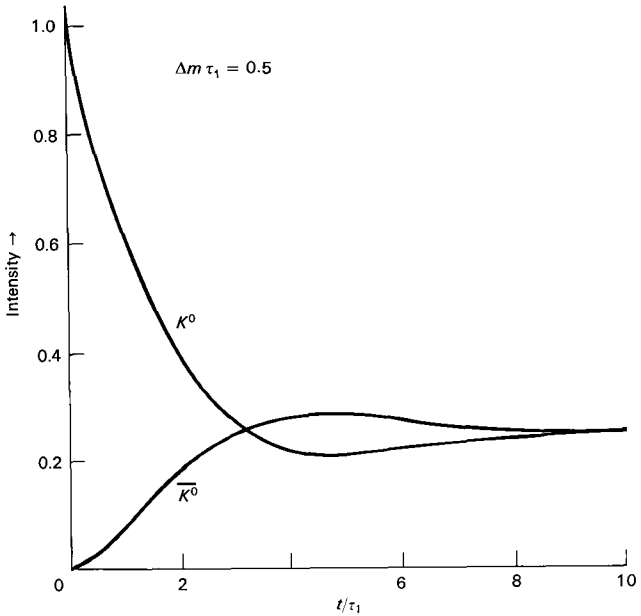

Fig. 4.32 Oscillations of K^0- and $\overline{K^0}$-intensities, for an initially pure K^0-beam, as calculated from Eqs. (4.61) and (4.62). A value $\Delta m \times \tau_1 = 0.5$ has been assumed.

number of $\overline{K^0}$ interaction events (i.e. the hyperon yield) as a function of position from the K^0-source, one can therefore deduce $|\Delta m|$, but not the sign. The first measurements (1962) of $|\Delta m|$ involved this method, and gave a value of order $1.5/\tau_1$, now known to be much too high. The currently accepted value is

$$\Delta m \times \tau_1 = 0.47 \pm 0.01, \tag{4.63}$$

where $\Delta m = m_2 - m_1$, and, as indicated in the next section, $m_2 > m_1$.

Using the value $\tau_1 = 0.86 \times 10^{-10}$ sec, (4.63) yields $(\Delta m)c^2 = 4 \times 10^{-6}$ eV, or a fractional $K_1 - K_2$ mass difference of

$$\frac{\Delta m}{m} = 10^{-14}. \tag{4.64}$$

The magnitude of the self-energy (i.e. contribution to the mass) of K_1 and K_2 can be estimated crudely by inspection of Fig. 4.33. (Incidentally, it is

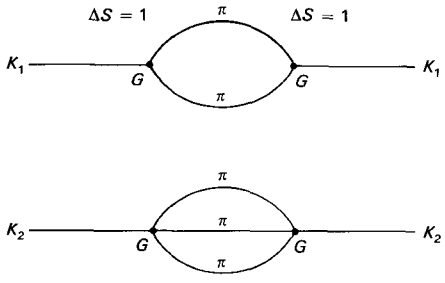

Figure 4.33

not known how to do a sophisticated calculation.) In the above diagrams the "weak" mass generated is clearly proportional to G^2 (all higher order terms being negligible in comparison), and thus to an effect of the second order in the weak coupling constant—the only one so far observed experimentally. Since $G = 10^{-5}/M_p^2$, we must introduce a mass in order to get the dimensions right. It is reasonable to choose this as the kaon mass. Since we have two strangeness-changing transitions, we should in fact replace G by $G \sin\theta_c$, θ_c being the Cabibbo angle. Hence we may estimate

$$\Delta m_K \text{ (for } \Delta S = 1 \text{ coupling)} \approx G^2 \times \sin^2\theta_c \times m_K^5 = 10^{-13} m_K = 10^{-4} \text{ eV}, \tag{4.65}$$

within an order of magnitude of the observed value (4.64). By a similar argument, one can set very stringent limits on the strength of a possible direct $\Delta S = 2$ transition between K^0- and $\overline{K^0}$-states. If fG denotes the coupling strength, then

$$\Delta m_K \text{(for } \Delta S = 2 \text{ coupling)} \approx fGm_K^3 = 10^3 f \text{ eV}, \tag{4.66}$$

giving $f \leqslant 10^{-8}$ from the observed value of Δm. Such an extremely weak coupling (called *superweak*) has been postulated in connection with *CP*-violation (Section 4.12).

4.11.3 Transmission Regeneration: the Sign of Δm

A measurement of the mass difference Δm can also be made by observations on the regenerated K_1-intensity as a function of regenerator thickness. The regenerated amplitude originates from the different K^0 and $\overline{K^0}$ nuclear scattering amplitudes, and three types of scattering can be considered; scattering from individual nucleons, scattering from an entire nucleus, and finally, coherent scattering from all nuclei in the regenerator slab, within the beam width. The latter is sometimes called "transmission regeneration," since it means that the K_2-beam is attenuated in passing through matter and gives rise to a *parallel* beam of K_1. Just as in optical diffraction, the transmission-regenerated K_1-beam will have an extremely small angular spread, $\Delta\theta \sim \lambda/d$, where λ is the kaon wavelength and d the slab diameter (i.e. the "slit width"). For example, for a 1 GeV/c kaon beam, $\lambda = 4 \times 10^{-14}$ cm, so that for $d = 20$ cm (as commonly used), $\Delta\theta = 10^{-15}$. In contrast, the regeneration angular distribution from the incoherent processes of individual nuclear scattering will have $\Delta\theta \sim \lambda/R$, where R is the nuclear radius, and would be of order 10^{-1} rad. Figure 4.34 shows how these different regeneration amplitudes can be resolved.

The principle of one experiment to measure the mass difference Δm is illustrated in Fig. 4.35. A K^+-beam of momentum 0.99 GeV/c impinges on a charge exchange target of copper, generating a beam of K^0-mesons. After traveling some distance, in which the bulk of the K_1-component decays, the predominantly K_2-beam enters a regenerator of iron. The parallel beam of K_1 at the rear of the regenerator then consists of a superposition of two amplitudes; ψ_S due to K_1 directly from the target; and ψ_R, the transmission-regenerated K_1-component from the iron slab. The K_1-intensity, I, is measured by observing decays $K_1 \to \pi^+\pi^-$ in spark chambers. $I = |\psi_S + \psi_R|^2$, depending on both magnitudes and relative phases of ψ_S and ψ_R. The phase of ψ_S depends on the distance from source to detector, and the wavenumber $k_1 = p_1$ of the direct K_1-component. The phase of ψ_R depends on the wavenumbers of both the K_2 and regenerated K_1, denoted by p_2 and p_1. These are not equal owing to the small mass difference; in fact, $\Delta p = p_1 - p_2 = m \times \Delta m/p$, where p and m are average values. The phase of ψ_R also depends on the inherent phase of the regenerated K_1-wave, relative to the incident K_2-wave, i.e. the phase of the quantity $f_{12} = (f - \bar{f})/2$ in (4.58). f_{12} can be found from data on $K^{\pm}p$ and $K^{\pm}n$ cross sections, and an optical model of the nucleus. Then the only unknown is Δm, which is measured by observing the change in the ψ_S/ψ_R interference as a function of distance L between source and regenerator. This is the principle of the method; the reader is referred to the original paper of Mehlhop *et al.* (1968) for the full algebraic detail.

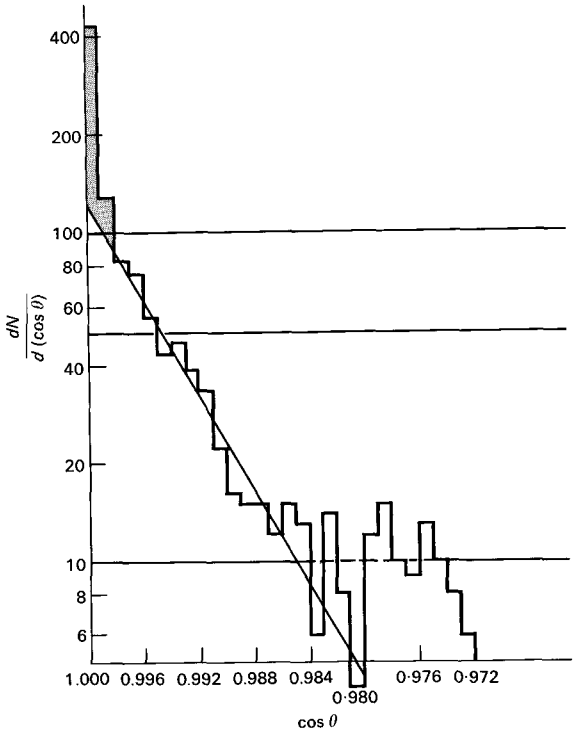

Fig. 4.34 Experimental results showing the transmission-regenerated peak (shaded) superimposed on the broader distribution due to nuclear (incoherent) regeneration (from experiment of Fig. 4.35).

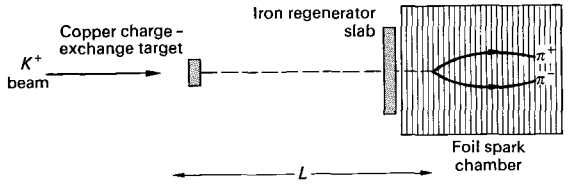

Fig. 4.35 Principle of experiment to determine the magnitude and sign of the $K_1 - K_2$ mass difference, by observing interference of the K_1-amplitude direct from a K^0-source, with that from regeneration by K_2 in an iron plate. (After Mehlhop *et al.*, 1968.)

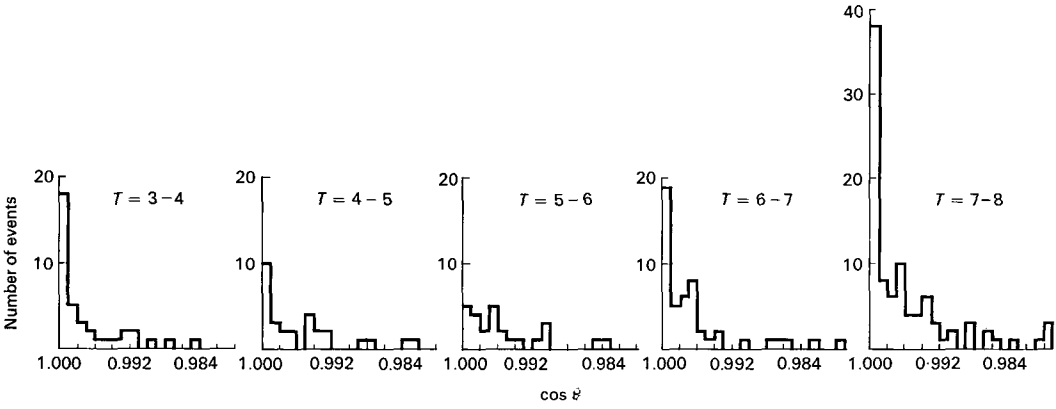

Fig. 4.36 Intensity of $K_1 \to 2\pi$ decay events plotted against $\cos\theta$, where θ is the angle between the K_1 momentum vector and the direction of the incident K_0-beam. As in Fig. 4.34, the forward peak ($\cos\theta > 0.998$) due to transmission regeneration is clearly visible. Note how the intensity of this peak varies with source-regenerator distance $T = L/\Lambda$ measured in units of K_1 mean lifetime, due to interference between direct and regenerated K_1-amplitudes.

Figure 4.36 shows how the forward intensity of 2π-decays fluctuates with L, expressed in terms of the proper time of flight $T = L/\Lambda$, where Λ is the mean decay length for K_1 of the beam momentum (4 cm in this case). The analysis of this data gave $\Delta m \times \tau_1 = 0.42 \pm 0.04$, and confirmed that $m_2 > m_1$ as in (4.63).

4.12 *CP*-VIOLATION IN K^0-DECAY

In 1964, the picture drawn above, of K^0 decay processes occurring through pure *CP*-eigenstates, K_1 and K_2, was changed by the observations by Christenson *et al.* and Abashian *et al.* that the long-lived K^0 could also decay to $\pi^+\pi^-$ with a branching ratio of order 10^{-3}. The experimental arrangement employed and results obtained are shown in Fig. 4.37. The nomenclature K_1 (for a state of $CP = +1$) and K_2 ($CP = -1$) has therefore been superseded by K_S (short-lived component) and K_L (long-lived component). The arguments quoted above on regeneration and mass difference, which follow from the superposition principle, remain essentially unchanged, although the formulae (4.56) need to be modified slightly if they are to describe K_S and K_L. The measure of the degree of *CP*-violation is usually quoted as the amplitude ratio

$$|\eta_{+-}| = \frac{\text{Ampl. } K_L \to \pi^+\pi^-}{\text{Ampl. } K_S \to \pi^+\pi^-} = (1.90 \pm 0.05) \times 10^{-3}. \qquad (4.67)$$

The state K_S still consists principally of a $CP = +1$ amplitude, but with a little $CP = -1$, and K_L conversely. The conclusion, that in K^0-decay invariance under the operation *CP* was really violated, when it was conserved

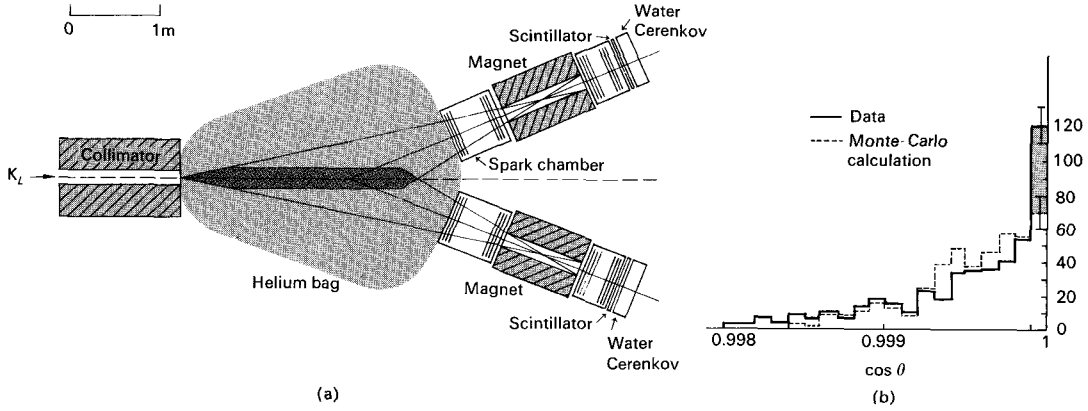

Fig. 4.37 (a) Experimental arrangement of Christenson *et al.* (1964) demonstrating the decay $K_L \to \pi^+\pi^-$. The K^0-beam is incident from the left, and consists of K_L only, the K_S-component having died out. K_L-decays are observed in a helium bag, the charged products being analyzed by two spectrometers, consisting of bending magnets and spark chambers triggered by scintillators. The rare 2-pion decays are distinguished from the common 3-pion and leptonic decays on the basis of the invariant mass of the pair, and the direction, θ, of their resultant momentum vector relative to the incident beam. (b) Cos θ distribution of events of $490 < M_{\pi\pi} < 510$ Mev. The distribution is that expected for 3-body decays (dotted line), but with some fifty events (shaded) exactly collinear with the beam due to the $\pi^+\pi^-$ decay mode.

in all other known interactions, was not finally accepted before exhausting all other possible explanations. Some of these were:

i) The effect is due to a new long-range galactic field, in which the potential energy of K^0 and $\overline{K^0}$ would be slightly different. This has the effect of making K_L and K_S a mixture of CP-eigenstates in a region where matter preponderates over antimatter. The rate for the decay $K_L \to 2\pi$ then turns out to be proportional to γ^{2J}, where $\gamma = (1 - v^2/c^2)^{-1/2}$ is the Lorentz factor of the kaon relative to the field (essentially the laboratory system), and J is the spin of the field quantum ($J = 1$ for a vector field). Experiments at different K_L-momenta rule this explanation out completely—there is no observed γ-dependence (Fig. 4.38).

ii) The argument $CP = +1$ for a $\pi^+\pi^-$ state depends on the assumption of Bose symmetry for the pions. Perhaps pions do not always obey Bose statistics. This argument was invalidated when the decay $K_L \to 2\pi^0$ was also observed, since $CP = +1$ for two identical, spinless particles regardless of statistics.

iii) The CP-eigenstate K_2 decays into K_1 plus an undetected particle S, lighter than the $K_L - K_S$ mass difference, and with $CP = -1$, i.e. $K_2 \to S + K_1 \to S + \pi^+ + \pi^-$. In such a situation, there could be no interference between the final state $\pi^+\pi^-S$ of K_2-decay, and $\pi^+\pi^-$ from decay of K_1 obtained by regeneration in a plate. As Fig. 4.39 indicates, interference between the K_L and K_S 2π-amplitudes is clearly demonstrated.

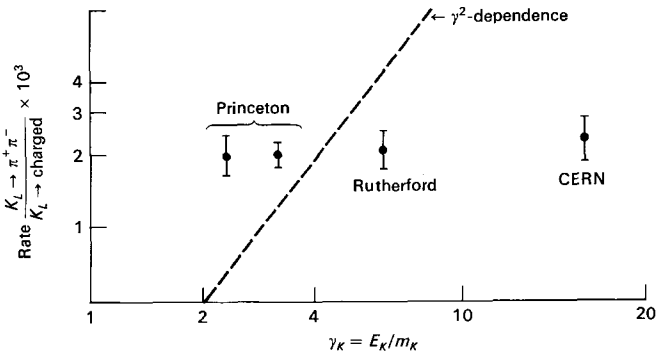

Fig. 4.38 Observed branching ratio for $K_L \to \pi^+\pi^-$ plotted as a function of K^0-momentum. Note the absence of any detectable momentum dependence.

Even more radical proposals, such as throwing doubt on the fundamental principle of superposition in wave mechanics, were advertised, but eventually one was left with the certain fact that *CP*-invariance really is violated in $K_L \to 2\pi$ decays. Subsequently, it was observed that the *leptonic* decay modes of K_L provided evidence for *CP*-noninvariance. These modes are

$$K_L \to e^+ \nu \pi^- \quad \text{or} \quad \mu^+ \nu \pi^-,$$

and

$$K_L \to e^- \bar{\nu} \pi^+ \quad \text{or} \quad \mu^- \bar{\nu} \pi^+, \tag{4.68}$$

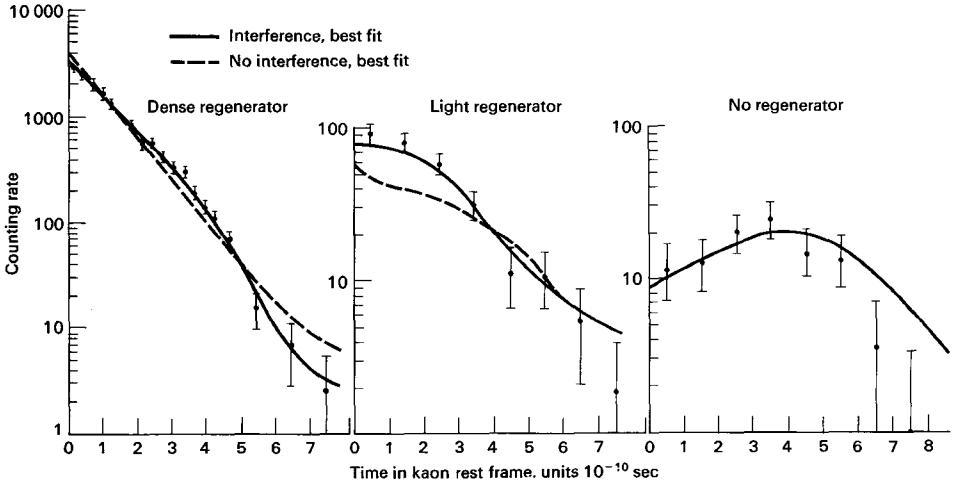

Fig. 4.39 Interference observed between the 2π final state from the *CP*-violating K_L-decay, and that from decay of K_S, the latter being produced by regeneration of the short-lived component in a plate. (After Alff-Steinberger *et al.*, 1966.)

where ν stands for ν_e or ν_μ, whichever is appropriate. The state $e\nu\pi$ is *not* a CP-eigenstate, in fact it is better described in terms of the K^0 and $\overline{K^0}$ strangeness eigenstates. By the $\Delta S/\Delta Q = +1$ rule (Section 4.8.2), the allowed decays are $K^0 \to e^+\nu\pi^-$ and $\overline{K^0} \to e^-\bar{\nu}\pi^+$. Nevertheless, the two decays (4.68) transform into one another under the CP-operation, and if CP-invariance is violated, one should obtain a small charge asymmetry. This has been detected, being

$$\delta = \frac{\text{Rate}\,(K_L \to e^+\nu\pi^-) - \text{Rate}\,(K_L \to e^-\bar{\nu}\pi^+)}{\text{Rate}\,(K_L \to e^+\nu\pi^-) + \text{Rate}\,(K_L \to e^-\bar{\nu}\pi^+)} = 2 \times 10^{-3}.$$

The source of the CP-violation is at present unknown. An important experiment in this connection is the precise determination of the ratio

$$\frac{K_L \to 2\pi^0}{K_L \to \pi^+\pi^-}. \tag{4.69}$$

For the short-lived component, the observed ratio

$$\frac{K_S \to 2\pi^0}{K_S \to \pi^+\pi^-} = 0.45 \pm 0.02. \tag{4.70}$$

This is nearly consistent with the value, $\frac{1}{2}$, expected from the $\Delta I = \frac{1}{2}$ rule. We recall that the two-pion state can have $I = 0$ or 2, and the $\Delta I = \frac{1}{2}$ rule allows $I = 0$ only. The Clebsch-Gordan coefficients for the addition of two isospin 1 particles then yield the above branching ratio. One method of accounting for the $K^+ \to \pi^+\pi^0$ decay ($I_{2\pi} = 2$) is to postulate an admixture of $\Delta I = \frac{3}{2}$ (or $\frac{5}{2}$) transitions (Section 4.8.1). For an $I = 2$ final state in $K^0 \to 2\pi$ decay, the expected value of the branching ratio (4.70) is 2, instead of $\frac{1}{2}$. Early measurements of the ratio (4.69) for the long-lived CP-violating decay suggested a value much greater than $\frac{1}{2}$. It was then plausible that the CP-violating amplitude was associated specifically with $\Delta I = \frac{3}{2}$ transitions. Later experiments have yielded lower values of the ratio; the average of these gives

$$|\eta_{00}| = \frac{\text{Ampl.}\,K_L \to 2\pi^0}{\text{Ampl.}\,K_S \to 2\pi^0} = (2.1 \pm 0.2) \times 10^{-3},$$

approximately equal to η_{+-} in (4.67). An example of a $K_L \to 2\pi^0$ decay event is shown in Fig. 4.40. It may be remarked that one theory predicts the ratios (4.69) and (4.70) to be identical. This is the *superweak theory* proposed by Wolfenstein (1964), in which the CP-violating amplitude arises exclusively from a new form of interaction obeying the selection rule $\Delta Q = -\Delta S$ and allowing $\Delta S = 2$. Comparing (4.65), (4.66) and inserting the observed CP-violating parameter η_{+-} (4.67), we see that the superweak coupling is of order 10^{-8} of the conventional weak coupling. Thus, there is probably no hope that it could be observed in any other physical process outside the extremely precise "interferometer" provided by the $K_L - K_S$ system.

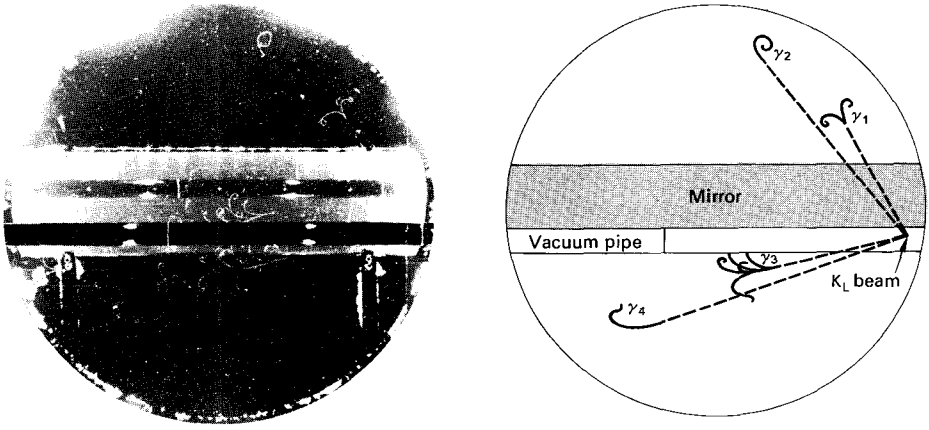

Fig. 4.40 Probable example of the decay $K_L \rightarrow 2\pi^0 \rightarrow 4\gamma$ obtained in an experiment to measure η_{00} in the CERN heavy liquid bubble chamber. The K_L-beam traverses a vacuum pipe through the chamber. γ-rays from the $2\pi^0$-mode are converted to e^+e^- pairs in the surrounding liquid (CF_3Br). Pairs occurring behind the pipe are rendered visible by a mirror at the rear of the chamber. (Courtesy, CERN Information Service.)

A general remark may be made in conclusion. Until the advent of *CP*-violation, there was no unambiguous way of defining left-handed and right-handed coordinate systems, or of differentiating matter from antimatter, on a cosmic scale. Thus, aligned Co^{60} nuclei emit negative electrons with forward-backward asymmetry and left-handed polarization (as we define left-handed). This is insufficient information to describe what we mean by a left-handed system, with the aid of light signals to an intelligent being in a distant part of the universe, unless one can also uniquely define negative and positive charge, or equivalently Co^{60} and anti-Co^{60}. *CP*-violation, however, provides an unambiguous definition. Positive charge is now defined as that of the lepton associated with the more abundant leptonic decay mode of the long-lived K_L-particle, $(K_L \rightarrow \pi^- e^+ \nu / K_L \rightarrow \pi^+ e^- \bar{\nu}) > 1$. This lepton has the same (or opposite) charge as the local atomic nuclei of matter (or antimatter).

BIBLIOGRAPHY

Feinberg, G., and L. Lederman, "Physics of muons and muon neutrinos," *Ann. Rev. Nucl. Science* **13,** 431 (1963).

Gasiorowicz, S., *Elementary Particle Physics*, John Wiley, New York, 1966.

Konopinski, E. J., "Experimental clarification of the laws of β-radioactivity," *Ann. Rev. Nucl. Science* **9,** 99 (1959).

Lederman, L., "Neutrino physics" in Burhop (ed.), *Pure and Applied Physics*, Academic Press, New York, 1967, Vol. 25-II.

Lee, T. D., and C. S. Wu, "Weak interactions," *Ann. Rev. Nucl. Science* **15,** 381 (1965).

Okun, L. B., *Weak Interactions of Elementary Particles*, Pergamon, London, 1965.

Prentki, J., "*CP* violation," and J. S. Bell and J. Steinberger, "Weak interactions of kaons," Proc. Oxford Conf. Elementary Particles 1965 (Rutherford High Energy Laboratory).

Reines, F., "Neutrino interactions," *Ann. Rev. Nucl. Science* **10,** 1 (1960).

Rubbia, C., "Weak interaction physics" in Burhop (ed.), *Pure and Applied Physics*, Academic Press, New York, 1968, Vol. 25-III.

PROBLEMS

4.1 Show that, if the neutrino in β-decay has mass m, the electron spectrum (4.2) has the form

$$N(p)\,dp = p^2(E_0 - E)^2\sqrt{1 - \left(\frac{mc^2}{E_0 - E}\right)^2}\,dp.$$

4.2 O^{14} has a half-life of 71 sec and an end-point energy $E_0 = 1.8$ MeV. The pion normally decays in the mode $\pi \to \mu + \nu$ with a mean life of 2.6×10^{-8} sec. Find the branching ratio for the decay

$$\pi^+ \to \pi^0 + e^+ + \nu \qquad (J^P = 0^- \to 0^-),$$

given that

$$m_{\pi^+} = 140 \text{ MeV}, \qquad m_{\pi^0} = 135 \text{ MeV}, \qquad m_e = 0.5 \text{ MeV}.$$

Only a *rough* estimate is required, so crude approximations may be used. [The observed ratio $(\pi^+ \to \pi^0 e^+ \nu/\pi^+ \to \mu^+ \nu) = 1.02 \times 10^{-8}$; you should get within a factor of 3 of this number.]

4.3 The neutron has a mean lifetime $\tau_n = 930$ sec, and the muon $\tau_\mu = 2.2 \times 10^{-6}$ sec. Show that the couplings involved in the two cases are of the same order of magnitude, when account is taken of the phase-space factors.

4.4 Obtain an estimate of the branching ratio $(\Sigma^- \to \Lambda e^- \bar{\nu})/(\Sigma^- \to n\pi^-)$, assuming that the matrix element for the electron decay is the same as that of the neutron, and that baryon recoil may be neglected. (See the Table in the preface for neutron and Σ-decay data.)

4.5 Strangeness-changing decays do not conserve isospin but appear to obey the $\Delta I = \frac{1}{2}$ rule. Use this rule to compute the ratios

i) $K_s \to \pi^+\pi^-/K_s \to \pi^0\pi^0$,

ii) $\Xi^- \to \Lambda\pi^-/\Xi^0 \to \Lambda\pi^0$.

Compare your answers with the experimental values in the Table in the preface. [*Hint:* the $\Delta I = \frac{1}{2}$ rule may be applied by postulating that a hypothetical particle of $I = \frac{1}{2}$—called a "spurion"—is added to the left-hand side in a weak decay process, and then treating the decay as an isospin-conserving reaction.]

4.6 What is the expected ratio $K_L \to 2\pi^0/K_L \to \pi^+\pi^-$ if the pions are in (i) an $I = 0$ state ($\Delta I = \frac{1}{2}$ rule), or (ii) an $I = 2$ state ($\Delta I = \frac{3}{2}$ or $\frac{5}{2}$)?

4.7 Using the $\Delta I = \frac{1}{2}$ rule, find a relation between the amplitudes for

$$\Sigma^+ \to n\pi^+, \quad \text{say } a_+,$$
$$\Sigma^- \to n\pi^-, \quad \text{say } a_-,$$
$$\Sigma^+ \to p\pi^0, \quad \text{say } a_0.$$

You will need to introduce $I = \frac{3}{2}$ and $I = \frac{1}{2}$ amplitudes. The triangle relation you should obtain is

$$a_+ + \sqrt{2}a_0 = a_-.$$

Experimentally, $|a_+| \approx |a_0| \approx |a_-|$, so that a right-angled triangle results.

4.8 Given that the width of the $N^*(1236)$ π-p resonance is 150 MeV, estimate the branching ratio for β-decay

$$\frac{N^{*++} \to p + e^+ + \nu}{N^{*++} \to p + \pi^+}.$$

4.9 How can one produce experimentally a beam of pure, monoenergetic K^0-particles? If a short pulse of such particles travels through a vacuum, compute the intensity of K^0 and $\overline{K^0}$ as a function of proper time, assuming the mass difference Δm equal to (i) $0.5/\tau_1$, (ii) $2/\tau_1$. Display the phenomena on a graph.

4.10 An experiment in a gold mine in South Dakota has been carried out to detect solar neutrinos, using the reaction

$$\nu + \mathrm{Cl}^{37} \to \mathrm{Ar}^{37} + e^-.$$

The detector contained approximately 4×10^5 liters of tetrachlorethylene (C_2Cl_4). Estimate how many atoms of Ar^{37} per day would be produced, making the following assumptions:

a) solar constant = 2 cal cm^{-2} min^{-1};

b) 10% of thermonuclear energy of sun appears in neutrinos, of mean energy 1 MeV;

c) 1% of all neutrinos are energetic enough to induce the above reaction;

d) the cross section per Cl^{37} nucleus for "active" neutrinos is 10^{-45} cm^2;

e) Cl^{37} isotopic abundance is 25%;

f) density C_2Cl_4 = 1.5 g ml^{-1}.

Do you expect any difference between day rate and night rate? [For description of the experiment, see R. Davis, D. S. Harmer, and K. C. Hoffman, *Phys. Rev. Lett.* **20,** 1205 (1968).]

4.11 Energetic neutrinos may produce single pions in the following reactions on protons and neutrons:

i) $\nu + p \to \pi^+ + p + \mu^-$,

ii) $\nu + n \to \left.\begin{matrix} \pi^0 + p \\ \pi^+ + n \end{matrix}\right\} + \mu^-$.

Assume the process is dominated by the first pion-nucleon resonance $N^*(1236)$, so that the π-nucleon system has $I = \frac{3}{2}$ only. As in weak decay processes of $\Delta S = 0$, the isospin

of the hadronic state then changes by one unit ($\Delta I = 1$ rule). Show that this rule predicts a rate for (i) three times that of (ii). Also show that, on the contrary, for a $\Delta I = 2$ transition (for which there is no present evidence), the rate for (ii) would be three times that for (i).

4.12 Use the $\Delta I = \frac{1}{2}$ rule to demonstrate the following relations between the rate of three-pion decays of charged and neutral kaons:

$$\Gamma(K_L \to 3\pi^0) = \tfrac{3}{2}\Gamma(K_L \to \pi^+\pi^-\pi^0),$$
$$\Gamma(K^+ \to \pi^+\pi^+\pi^-) = 4\Gamma(K^+ \to \pi^+\pi^0\pi^0),$$
$$\Gamma(K_L \to \pi^+\pi^-\pi^0) = 2\Gamma(K^+ \to \pi^+\pi^0\pi^0).$$

[Comment: These results depend on the (reasonable) assumption that the three pions are in a relative S-state. Then, any pair of pions must be in a symmetric isospin state, i.e. $I = 0$ and/or 2. The third pion ($I = 1$) must then be combined with the pair to yield a three-pion state of $I = 1, I_3 = 1$ for K^+, or $I = 1, I_3 = 0$ for K^0 (from the $\Delta I = \frac{1}{2}$ rule). It is necessary to write the three-pion wave function in a manner which is, as required for identical bosons, completely symmetric under pion label interchange. Thus, the $\pi^+\pi^+\pi^-$ state must be written

$$(++-) = \frac{1}{\sqrt{6}}(\pi_1^+\pi_2^+\pi_3^- + \pi_2^+\pi_1^+\pi_3^- + \pi_3^-\pi_2^+\pi_1^+ + \pi_3^-\pi_1^+\pi_2^+ + \pi_2^+\pi_3^-\pi_1^+ + \pi_1^+\pi_3^-\pi_2^+).$$

Each term in this expression will be the product of an isospin state of $I = 0$ or 2, for the first two pions, and one of $I = 1$, for the third pion, with appropriate Clebsch-Gordan coefficients.]